ARL 64-49, PART II
DECEMBER 1964

Aerospace Research Laboratories

BASIC RESEARCH ON GAS FLOWS THROUGH ELECTRIC ARCS - THE RADIATING ARC COLUMN

G. L. MARLOTTE
R. L. HARDER
R. W. PRICHARD
ELECTRO-OPTICAL SYSTEMS, INC.
PASADENA, CALIFORNIA

OFFICE OF AEROSPACE RESEARCH
United States Air Force

NOTICES

When Government drawings, specifications, or other data are used for any purpose other than in connection with a definitely related Government procurement operation, the United States Government thereby incurs no responsibility nor any obligation whatsoever; and the fact that the Government may have formulated, furnished, or in any way supplied the said drawings, specifications, or other data, is not to be regarded by implication or otherwise as in any manner licensing the holder or any other person or corporation, or conveying any rights or permission to manufacture, use, or sell any patented invention that may in any way be related thereto.

- - - - - - - - - -

Qualified requesters may obtain copies of this report from the Defense Documentation Center, (DDC), Cameron Station, Alexandria, Virginia.

- - - - - - - - - -

This report has been released to the Office of Technical Services, U. S. Department of Commerce, Washington 25, D. C. for sale to the general public.

- - - - - - - - - -

Copies of ARL Technical Documentary Reports should not be returned to Aerospace Research Laboratories unless return is required by security considerations, contractual obligations or notices on a specified document.

500 - January 1965 - 448-24-542

ARL 64-49, PART II

BASIC RESEARCH ON GAS FLOWS THROUGH ELECTRIC ARCS – THE RADIATING ARC COLUMN

G. L. MARLOTTE
R. L. HARDER
R. W. PRICHARD

ELECTRO-OPTICAL SYSTEMS, INC.
PASADENA, CALIFORNIA

DECEMBER 1964

Contract AF 33(657)-7940
Project 7063
Task 7063-03

AEROSPACE RESEARCH LABORATORIES
OFFICE OF AEROSPACE RESEARCH
UNITED STATES AIR FORCE
WRIGHT-PATTERSON AIR FORCE BASE, OHIO

FOREWORD

This interim technical report was prepared by Electro-Optical Systems, Inc., Pasadena, California, on Contract AF 33(657)-7940 for the Aerospace Research Laboratories, Office of Aerospace Research, United States Air Force. The research reported herein was accomplished on Task 7063-03, "Energy Exchange Phenomena in Electric Arc Discharges" of Project 7063, "Mechanics of Flight" under the technical cognizance of Mr. Charles A. Davies of the Thermo-Mechanics Research Laboratory of ARL.

ABSTRACT

Simple analytic expressions are derived for describing the radiation from an arc confined in a cylindrical constrictor and operating in the general "gas-heating" or "inlet" regime. These expressions were obtained by postulating linear relationships among the plasma properties σ, u and ϕ, the electrical conductivity, the power radiated per unit volume, and the thermal conductivity integral $\int_0^T K dt$, respectively. For initial comparisons, radiation from "fully developed" arcs in argon and nitrogen has been measured as a function of the arc current and the gas pressure in the confining cylinder. These measurements are compared to the appropriate limit in the analytical predictions and the correlation is found to be good, except for the electric field dependence upon current. It has been found possible to improve the correlation by modifying the results of the analysis to include, in an approximate manner, the nonlinear relationships that actually exist among the properties of the plasma. Similarity parameters, which are inferred from the analysis and approximately derived from the basic equations, are applied successfully to the measurements with argon and nitrogen and to extensive calculations with nitrogen. Radiation measurements for comparison with the complete analysis remain to be accomplished in the "gas heating" or "inlet" regime, but the work to date offers hope that the analysis has included the main features of the arc-gas interaction.

TABLE OF CONTENTS

LIST OF ILLUSTRATIONS

LIST OF ILLUSTRATIONS (CONT'D)

LIST OF SYMBOLS

All quantities are in MKS units

E	Electric Field
h	Enthalpy
I	Total Arc Current
j	Current Density
K	Thermal Conductivity
p	Gas Pressure
P_{cond}	Power Conducted to Walls per Unit Length
P_{rad}	Power Radiated to Walls per Unit Length
u	Radiated Power per Unit Volume
r	Radial Coordinate
R	Radius of Cylinder
T	Gas Temperature
w	Axial Gas Velocity
z	Axial Coordinate
ξ	Ratio of Radiated Power to Conducted Power
ρ	Gas Density, Nondimensional Radius = r/R
σ	Electrical Conductivity
ϕ	Thermal Conductivity Integral
Φ, Φ'	Similarity Functions for Radiation
Ψ, Ψ'	Similarity Functions for Arc Characteristic

Subscripts

1	Denotes value of quantity at which the approximations to σ and u vanish.
a	Evaluated at atmospheric pressure.

1. INTRODUCTION

The new technologies of hypersonic flight, space flight, rocketry and light sources, as well as some aspects of nuclear fission and fusion work, have created several new requirements for sources of hot gas or plasma above the combustion temperature regime. Thus, the heating of various gases by means of electric arcs, typically to temperatures between 3000 ^{o}K and 50,000 ^{o}K or higher, at pressures of from 1 atmosphere to several hundred atmospheres, has become an important technology, resulting in many specialized forms of arc plasma sources, or arcjet devices. At these pressures and temperatures, the power that is radiated per unit volume from the gas can become the major component of heat transfer in the gas. Techniques must be devised for properly incorporating this phenomenon into the design concepts of arc heater and arc light source devices.

Considerable theoretical work has been done in an attempt to compute the power radiated per unit volume from the gas as a function of the gas temperature and pressure[1, 2]. There is general agreement that the major portion of the radiation results from a combination of two types of radiative transitions of "free" plasma electrons. The well-known bremsstrahlung continuum results from electrons being deflected by coulomb interactions with positive ions and transforming kinetic energy into radiation; added to this radiation is that due to radiative

---

Manuscript released by the authors 3 June 1964 for publication as an ARL Technical Documentary Report.

recombinations of electrons into capture orbits. An equation describing these two processes and which allows computation of the power radiated by the gas in terms of known physical constants has been derived by Unsold[3] using the classical Kramers theory. Yos[1] has further corrected this formula to match very limited experimental data, and has computed and plotted the power radiated per unit volume for a number of gases as a function of temperature and pressure.

Because of the rather approximate nature of the calculations, which may well allow an error in the absolute magnitude of a factor of 3 or greater, it is highly desirable to carry out experiments involving the measurement of radiation. It has been found that, in practice, experiments are very difficult, and progress has been quite slow in finding techniques that will allow a simple one-to-one comparison between theory and experiment including radiation. In this report, one approach, with some preliminary results, is discussed in detail. Here the radiation is from argon and nitrogen, heated by an arc in a confining cylinder. The pressure and cylinder diameter are maintained at values such that the gas should be "optically thin," i.e., a negligible amount of self-absorption occurs. Analytical and experimental results are then compared on the basis of parameters derived from linearized approximations in the theory and from similarity considerations.

2. APPROACH

The configuration that has been chosen for the detailed study of the radiation from the gas is shown schematically in Fig. 1*. In the correlation between theory and experiment, it is assumed that the gas flow rate through the cylinder is low enough so that all of the power dissipated in the discharge is transferred to the segment walls by conduction and radiation. However, in formulating the analysis it is desirable to be able also to describe the region where the gas is being heated, so that eventually the parameters of the heater, e. g., constrictor length and diameter, can be specified. This requires that an attempt be made to solve the steady-state energy equation with variation in both the axial and radial dimensions. In order to obtain simple analytical solutions which are very desirable, linear relations are postulated among the quantities ϕ, σ, and u, where ϕ is the thermal conductivity integral, σ is the electrical conductivity, and u is the power radiated per unit volume of gas. Such linear relations can be expected to hold only over very limited ranges of temperature.[1] However, useful relations and parameters may be obtained from the linearized solution which might then suggest the formulation of more general

---

* This classical "Maecker-type"[4] column, and the measurements and theory associated with it are detailed or referenced.[2,5]

similarity parameters that have a much wider range of application than would the linear solution itself. Another point of view can also be adopted such that the linear relations are only average values of the essentially nonlinear relations among the variables. Once the solution is obtained, these average values can then be replaced by a more accurat nonlinear relation in the solution. The validity of this procedure can best be checked by self-consistent comparisons between the experimental results and the "modified" solution. This comparison is carried out in the following sections.

3. LINEARIZED ANALYSIS

An approximate solution is known for the axial and radial distribution of gas properties in the steady flow of a gas in a cylinder with an axial electric arc.[6] The theory will be expanded to include radiation in the gas.

The enthalpy equation states that, for steady flow, the net rate of heat outflow from a unit volume by conduction, convection and radiation is equal to the power input due to ohmic heating. If radial convection and axial conduction are neglected, the equation in cylindrical coordinates is:

$$\frac{\partial}{\partial z}(\rho w h) + \left[-\frac{1}{r}\frac{\partial}{\partial r}\left(r\frac{\partial \phi}{\partial r}\right) + u \right] = \frac{j^2}{\sigma} \qquad (1)$$

where

ϕ = thermal conductivity integral, $\phi = \int_0^T K dT$

u = power radiated per unit volume (self-absorption neglected)

The following approximate solution is valid for the "gas heating" or "entrance" region for which the arc (conducting region) does not fill the cylinder.

Assume that ρw is constant, which implies the neglecting of radial flow. Assume that

$$h = h_1 + \left\langle \frac{dh}{d\phi} \right\rangle (\phi - \phi_1)$$

where $\left\langle \frac{dn}{d\phi} \right\rangle$ is a function of pressure only.

Assume that σ is zero for ϕ less than ϕ_1 and $\sigma = \left\langle \frac{d\sigma}{d\phi} \right\rangle_a \left(\frac{p}{p_a} \right)^s (\phi - \phi_1)$ for ϕ greater than ϕ_1, where $\left\langle \frac{d\sigma}{d\phi} \right\rangle_a$ is a constant evaluated at atmospheric pressure (for convenience).

By using the fact that the integral of the current density j over the cross section is the total current I, and assuming that the electric field $E = j/\sigma$ is independent of radial position, we can write:

$$j^2/\sigma = I^2\sigma \Big/ \left[\int_0^R \sigma \, 2\pi r \, dr \right]^2$$

All of the above assumptions are essentially the same as those made by Stine and Watson [6] except for the explicit inclusion of the pressure dependence of σ; the pressure dependence is likely to be small but is included for later reference.

The radiation u in Eq. (1) is the net power radiated per unit volume. Assume that the column is optically thin, and hence that the self-absorption by the gas can be neglected. We assume that the total specific radiation, u, is zero for ϕ less than ϕ_1, and

$$u = \left\langle \frac{du}{d\phi} \right\rangle_a \left(\frac{p}{p_a} \right)^t (\phi - \phi_1)$$

for ϕ greater than ϕ_1, where $\left\langle \frac{du}{d\phi} \right\rangle_a$ is a constant evaluated (again, for convenience only) at atmospheric pressure. The value of ϕ_1 in the above assumptions is obtained by extrapolating the straight line approximations between σ and ϕ and between u and ϕ (at atmospheric pressure

to the ϕ axis and adjusting them so that the same value of ϕ_1 is obtained from the two lines. The value of $r(= r_1)$ corresponding to ϕ_1 then defines an "effective arc radius." Actual values for $\sigma(\phi)$ and $u(\phi)$ may be obtained, for example, from the data given or quoted[1, 5, 7] for various gases.

With the above assumptions, Eq. 1 becomes:

$$\rho w \left\langle \frac{dh}{d\phi} \right\rangle \frac{\partial(\phi-\phi_1)}{\partial z} - \frac{1}{r}\frac{\partial}{\partial r}\left(r \frac{\partial(\phi-\phi_1)}{\partial r}\right) + \left\langle \frac{du}{d\phi} \right\rangle_a \left(\frac{p}{p_a}\right)^t (\phi-\phi_1)$$

$$= \frac{I^2 (\phi-\phi_1)}{\left\langle \frac{d\sigma}{d\phi} \right\rangle_a \left(\frac{p}{p_a}\right)^s \left[2\pi \int_0^{r_1} (\phi-\phi_1)\, r\, dr\right]^2} \tag{2}$$

for $r \le r_1$, and

$$\rho w \left\langle \frac{dh}{d\phi} \right\rangle \frac{\partial(\phi-\phi_1)}{\partial z} - \frac{1}{r}\frac{\partial}{\partial r}\left(r \frac{\partial(\phi-\phi_1)}{\partial r}\right) = 0 \tag{3}$$

for $r > r_1$.

The solution of Eq. (2) for $\phi = \phi_1$ at $r = r_1$ and $z = 0$ is

$$\phi-\phi_1 = \frac{I\, J_o\,(2.4\, r/r_1)\, f\,(z)}{2\pi J_1(2.4)\, r_1 \left\langle \frac{d\sigma}{d\phi} \right\rangle_a^{1/2} \left(\frac{p}{p_a}\right)^{s/2} \left[\frac{1}{4} + \left(\frac{r_1}{2.4}\right)^2 \left\langle \frac{du}{d\phi} \right\rangle_a \left(\frac{p}{p_a}\right)^t\right]^{1/2}} \tag{4}$$

where

$$f(z) = \left[1 - \exp\left\{-2(2.4)^2 z \left[\frac{1}{4} + \left(\frac{r_1}{2.4}\right)^2 \left\langle \frac{du}{d\phi} \right\rangle_a \left(\frac{p}{p_a}\right)^t\right] \Big/ \rho w r_1^2 \left\langle \frac{dh}{d\phi} \right\rangle\right\}\right]^{1/2}$$

Notice that even when radiation is included, the solution takes the form of a product solution; thus the solution at any radius is the product of a function of r with a function of z.

Eq. (5) may be written in the following form:

$$f(z) = (1 - e^{11.5\, z/z_o})^{1/2} \tag{6}$$

where

$$z_o = \frac{(\rho w)\, r_1^2 \left\langle \frac{dh}{d\phi} \right\rangle}{1 + \left(\frac{r_1}{2.4}\right)^2 \left\langle \frac{du}{d\phi} \right\rangle_a \left(\frac{p}{p_a}\right)^t} \tag{7}$$

If we write $(\rho w) = \frac{\dot{m}}{\pi R^2}$ where $\dot{m}$ is the mass flow rate,

$$\left\langle \frac{dh}{d\phi} \right\rangle = \left\langle \frac{dh}{d\phi} \right\rangle_a \left(\frac{p}{p_a}\right)^q ,$$

and

$$\xi = \left(\frac{r_1}{2.4}\right)^2 \left\langle \frac{du}{d\phi} \right\rangle_a \left(\frac{p}{p_a}\right)^t ,$$

then

$$z_o = \frac{\dot{m}}{\pi}\left(\frac{r_1}{R}\right)^2 \frac{\left\langle \frac{dh}{d\phi} \right\rangle_a \left(\frac{p}{p_a}\right)^q}{(1+\xi)} \tag{8}$$

In brief, the <u>axial</u> dependence of the various quantities will remain the same as in the original calculations of Stine-Watson[6] provided that the quantity z_o is now given by Eqs. (7), (8). As a result, it will suffice to consider only the radial dependence in the following discussion.

The complete radial dependence of ϕ (i.e., the asymptotic value for large z) is

$$(\phi-\phi_1) = \frac{I\, J_o\,(2.4\, r/r_1)}{2\pi\, J_1(2.4)\, r_1 \left\langle \frac{d\sigma}{d\phi} \right\rangle_a^{1/2} \left(\frac{p}{p_a}\right)^{s/2} \left[1 + \left(\frac{r_1}{2.4}\right)^2 \left\langle \frac{du}{d\phi} \right\rangle_a \left(\frac{p}{p_a}\right)^t\right]^{1/2}} \qquad 0 \le r \le r_1 \tag{9}$$

or

$$(\phi-\phi_1) = \frac{-2.4\, I\, \ln\,(r/r_1)}{2\pi r_1 \left\langle \frac{d\sigma}{d\phi} \right\rangle_a^{1/2} \left(\frac{p}{p_a}\right)^{s/2} \left[1 + \left(\frac{r_1}{2.4}\right)^2 \left\langle \frac{du}{d\phi} \right\rangle_a \left(\frac{p}{p_a}\right)^t\right]^{1/2}} \qquad r_1 < r \le R \tag{10}$$

where the "outer solution" (no ohmic heating or radiation) was found by setting $\partial\phi/\partial z = 0$ and matching $\partial\phi/\partial r$ with the "inner solution."

To initially compare the predictions of the linear theory with experimental measurements, only the asymptotic arc column region with the solution given in Eqs. (9, 10) will be considered. (No experimental data including radiation measurements are available for the inlet region as yet.)

For later reference, the complete predictions of the theory applied to the asymptotic arc column regime are listed below:

Ratio of total power radiated per unit length to total power conducted per unit length, ξ

$$\xi = \frac{P_{rad}}{P_{cond}} = \left(\frac{r_1}{2.4}\right)^2 \left\langle \frac{du}{d\phi} \right\rangle_a \left(\frac{p}{p_a}\right)^t \tag{11}$$

Total power radiated per unit length, P_{rad}

$$P_{rad} = \frac{2.4}{\left\langle \frac{d\sigma}{d\phi} \right\rangle_a^{1/2}} \xi \frac{I \left(\frac{p_a}{p}\right)^{s/2}}{r_1\, (1+\xi)^{1/2}} \tag{12}$$

Total power conducted per unit length, P_{cond}

$$P_{cond} = EI - P_{rad} = \frac{2.4}{\left\langle \frac{d\sigma}{d\phi} \right\rangle_a^{1/2}} \quad \frac{I\left(\frac{P_a}{p}\right)^{s/2}}{r_1 (1 + \xi)^{1/2}}$$

Thermal conductivity integral, ϕ

$$\phi - \phi_1 = \frac{J_o(2.4\ r/r_1)}{2\pi J_1(2.4) \left\langle \frac{d\sigma}{d\phi} \right\rangle_a^{1/2}} \quad \frac{I\left(\frac{P_a}{p}\right)^{s/2}}{r_1 (1 + \xi)^{1/2}} \quad 0 \le r \le r_1$$

$$\phi - \phi_1 = \frac{-2.4 \ln (r/r_1)}{2\pi \left\langle \frac{d\sigma}{d\phi} \right\rangle_a^{1/2}} \quad \frac{I\left(\frac{P_a}{p}\right)^{1/2}}{r_1 (1 + \xi)^{1/2}} \quad r_1 < r \le R$$

or

$$\phi = \frac{2.4 \ln (R/r)}{2\pi \left\langle \frac{d\sigma}{d\phi} \right\rangle_a^{1/2}} \quad \frac{I\left(\frac{P_a}{p}\right)^{s/2}}{r_1 (1 + \xi)^{1/2}} \quad r_1 < r \le ?$$

Electric field parameter, ER

$$ER = \frac{2.4}{\left\langle \frac{d\sigma}{d\phi} \right\rangle_a^{1/2}} \left(\frac{R}{r_1}\right) \cdot \frac{(1 + \xi)^{1/2}}{\left(\frac{p}{P_a}\right)^{s/2}}$$

Total current parameter, I/R

$$I/R = 2\pi J_1(2.4) \left\langle \frac{d\sigma}{d\phi} \right\rangle_a^{1/2} (\phi_{axis} - \phi_1) \quad \frac{(1 + \xi)^{1/2}}{(R/r_1)\left(\frac{P_a}{p}\right)^{s/2}}$$

"Radius of arc," r_1

$$R/r_1 = \exp\left[\frac{\phi_1}{2.4\ J_1(2.4)\ (\phi_{axis} - \phi_1)}\right] \tag{19}$$

$$= \exp\left[\frac{2\pi\ \phi_1\ (1 + \xi)}{EI}\right] \tag{20}$$

Average gas enthalpy, h_{avg}

$$h_{avg} - h_1 = \frac{\left\langle \frac{dh}{d\phi} \right\rangle_a}{\pi} \frac{\left(\frac{p}{p_a}\right)^q 2.4}{\left\langle \frac{d\sigma}{d\phi} \right\rangle_a^{1/2}} \frac{I\left(\frac{p_a}{p}\right)^{s/2}}{r_1(1+\xi)^{1/2}} \left\{\left(\frac{r_1}{2.4R}\right)^2 - \frac{\ln\ (R/r_1)}{2} + \frac{1-\left(\frac{r_1}{R}\right)^2}{4}\right\} \tag{21}$$

Wall heat load per unit area, q_w

$$q_w = \frac{EI}{2\pi R} = \frac{1}{2\pi R} \frac{2.4}{\left\langle \frac{d\sigma}{d\phi} \right\rangle_a^{1/2}} \frac{I}{r_1}\left(\frac{p_a}{p}\right)^{s/2} (1 + \xi)^{1/2} \tag{22}$$

The last two quantities are listed above for completeness, and will not be dealt with further except to mention that for $r_1 \approx R$ the maximum average enthalpy per unit heat load occurs when $\xi = 1$, or when the power radiated is equal to the power conducted.

4. EXPERIMENTAL RESULTS

A series of measurements were made with both argon and nitrogen in the asymptotic or fully developed discharge regime. The apparatus (Fig. 1) consisted of a "Maecker type"[4] stack of seven water cooled copper segments of 0.5 cm thickness, separated by insulating washers of 0.1 cm thickness. The internal hole diameter in the stack, through which the arc was drawn, was 0.50 cm. A special segment incorporating a quartz window was constructed and installed midway in the stack of segments for measuring the power radiated per unit length from the arc column. Detailed information on the device and the measurement techniques may be found in[5].

Arc characteristic measurements (electric field as a function of current), taken at 1.0 atmosphere pressure, are presented in Figs. 2 and 3 with the measurements of Maecker[4]. Figures 4 and 5 show the power radiated per unit length as a function of current at 1.0 atmosphere pressure, again with the measurements of Maecker[4]. The electric field as a function of pressure for I = 200 amperes current is plotted on Figs. 6 and 7 while Figs. 8 and 9 show the power radiated per unit length as a function of pressure for the same current.

A detailed comparison may now be made between the experimental measurements and the predictions of the simple theory (listed in Section 3, Eqs. (11) to (20) inclusive).

First, in order to apply the theory, values for certain constants must be obtained from curves of argon and nitrogen plasma properties. From Figs. 10 and 11, the following values were determined for the constants in the linear theory:

Argon			Nitrogen		
ϕ_1	=	300	ϕ_1	=	6000
$\left\langle \frac{d\sigma}{d\phi} \right\rangle_a$	=	1.76	$\left\langle \frac{d\sigma}{d\phi} \right\rangle_a$	=	0.428
$\left\langle \frac{du}{d\phi} \right\rangle_a$	=	3.38×10^5	$\left\langle \frac{du}{d\phi} \right\rangle_a$	=	0.720×10^5

(23)

(All MKS)

In addition, s was taken to be zero, and t was assigned a value of 1.0 for lack of better information. The predictions of the linear theory may now be calculated and drawn on Figs. 2 to 9. The radius ratio at first sight appears to be implicitly buried in the equations, but may be easily calculated and included in the plots as follows:

1. Assign values to $\dfrac{I}{r_1 (1 + \xi)^{1/2}} \left(\dfrac{\rho_a}{\rho}\right)^{s/2}$
2. Multiply each by $2.4 \left\langle \frac{d\sigma}{d\phi} \right\rangle_a^{1/2}$ from Eq. (17), yielding $EI/(1+\xi)$
3. Calculate R/r_1 from Eq. (20) and ξ for each pressure from Eq. (11)
4. All quantities in Figs. 2 to 9 may now be calculated from the appropriate equations. (For the constant current plots of Figs. 6, 7, 8, and 9, a simple cross-plotting is needed.)

In general, it may be seen that the current and pressure dependence of the radiated power from the linear theory agrees reasonably well with experiments (Figs. 4, 5, 8, 9); however, the prediction of the electric field as a function of current does not agree even qualitatively with the experiments as shown on Figs. 2 and 3. This disparity suggests that the nonlinear nature of the electrical conductivity curve given on Fig. 10 is quite important for the calculation of the electric field. Finally, after allowance is made for the current dependence disparity in Figs. 2 and 3, the electric field dependence upon the pressure, presented in Figs. 6 and 7 again correlates reasonably well between theory and experiment.

5. SIMILARITY CONSIDERATIONS

Up to this point, the linear theory has been compared with experiments and found to correlate reasonably well except for the electric field dependence upon current. In an attempt to account for this current dependence, it is suggested that the parameter $\left\langle \frac{d\sigma}{d\phi} \right\rangle_a$ in Eq. (17) might now be allowed to vary with $(\phi - \phi_1)$, because from Eq. (18), $(\phi - \phi_1)$ is related to the current. A similar process may be carried out with the $\left\langle \frac{du}{d\phi} \right\rangle_a$ parameter and the following similarity forms are obtained:

$$\frac{ER\left(\frac{p}{p_a}\right)^{s/2}}{(1+\xi)^{1/2}}\left(\frac{r_1}{R}\right) = \Psi\left\{\frac{I\left(\frac{p_a}{p}\right)^{s/2}}{R\,(1+\xi)^{1/2}}\left(\frac{R}{r_1}\right)\right\} \tag{24}$$

and

$$\frac{P_{rad}}{R^2}\left(\frac{p_a}{p}\right)^{t}\left(\frac{R}{r_1}\right)^{2} = \Phi\left\{\frac{I\left(\frac{p_a}{p}\right)^{s/2}}{R\,(1+\xi)^{1/2}}\left(\frac{R}{r_1}\right)\right\} \tag{25}$$

In order to convert these expressions into forms in which experimental results may be conveniently plotted, an expression is needed for R/r_1.

Now, R/r_1 can be written (see Eq. 20) from the linear theory as

$$\frac{R}{r_1} = \exp\left\{\frac{2\pi\phi_1}{\dfrac{ER\left(\frac{r_1}{R}\right)\left(\frac{p}{p_a}\right)^{s/2}}{(1+\xi)^{1/2}}\;\dfrac{I\left(\frac{R}{r_1}\right)\left(\frac{p_a}{p}\right)^{s/2}}{R\,(1+\xi)^{1/2}}}\right\} \tag{26}$$

Equation (26) with Eq. (24) indicates that

$$\frac{R}{r_1} = \frac{R}{r_1}\left\{\frac{I\left(\frac{p_a}{p}\right)^{s/2}}{R\,(1+\xi)^{1/2}}\right\} \tag{27}$$

and thus that

$$\frac{ER\left(\frac{p}{p_a}\right)^{s/2}}{(1+\xi)^{1/2}} = \psi'\left\{\frac{I\left(\frac{p_a}{p}\right)^{s/2}}{R\,(1+\xi)^{1/2}}\right\} \tag{28}$$

and

$$\frac{P_{rad}}{R^2}\left(\frac{p_a}{p}\right)^t = \phi'\left\{\frac{I\left(\frac{p_a}{p}\right)^{s/2}}{R\,(1+\xi)^{1/2}}\right\} \tag{29}$$

The similarity form of Eqs. (28) and (29) may also be obtained directly from the energy equation using an approximation technique (see Appendix A for details). All quantities can be measured now and the ranges of validity (if any) of Eqs. (28) and (29) can be checked.

Using the variables of Eq. (28), Fig. 12 presents all of the experimental data taken at 1.0 atmosphere or above in the present investigation for argon, including runs at different pressures and wall radii (s is taken to be zero). For some of the operating conditions, the power radiated was several times the power conducted with large increases in the electric field. An empirical expression was used for ξ in order to plot the R = 0.377 cm data since radiation was not measured at the time. No data below 1.0 atmosphere were plotted because there is some reason to believe that other effects become important that are not contained in the simple theory upon which the similarity parameters are based (non-equilibrium, for example). A corresponding plot for nitrogen is given in Fig. 13.

Turning now to Eq. (29), Fig. 14 plots some experimental data for argon. The pressure dependence of t = 1.0 is satisfactory, but the absolute value of the present measurements should not be taken too seriously as problems of window contamination were present at the time the data were taken.

On the other hand, the measurements with nitrogen on Fig. 15 were taken after the window contamination problem had been solved and agree quite well with those of Maecker. Again the pressure dependence of t = 1.0 is satisfactory.

In addition to using actual experimental results to check the similarity forms of Eqs. (28) and (29), "exact" calculations covering a much wider range of variables may be used. For example, extensive calculations on nitrogen[1] are reduced using similarity variables in Appendix A, with very convincing results. Some results of this reduction are sketched in on Figs. 13 and 15 for comparison purposes.

Up to this point in the discussion, the question implicitly dealt with has been "Can one collapse data taken over a wide range of operating conditions to a common basis?". The tentative results of Figs. 12, 13, 14, 15, and the plots of Appendix A, are quite encouraging in this regard but await the taking of considerably more experimental data.

From an engineering point of view, one can ask the following question: "To what extent can one predict the results of operation under a wide range of conditions using simple formulas, and not resorting to complex (or computer) calculations?". The manner in which the present "modified linear theory" may attempt an answer to the latter question is briefly discussed below.

Assume that $\sigma(\phi, p)$ and $u(\phi, p)$ are given. Essentially, in the present formulation, there exists a correspondence between

the shapes of the Ψ curve in Eq. (24) and $\sigma(\phi, p_a)$, and between the Φ curve in Eq. (25) and $u(\phi, p_a)$. This correspondence arises because the similarity rules defined by Ψ and Φ were first suggested by allowing $\left\langle \frac{d\sigma}{d\phi} \right\rangle_a$ and $\left\langle \frac{du}{d\phi} \right\rangle_a$, the constant slopes of the original linear approximations, to now vary with $(\phi - \phi_1)$ in the solutions.

As an example, if one assumes the following forms for Ψ and Φ:

$$\Psi(x) = C_1 x^n \tag{30}$$

$$\Phi(x) = C_2 x^m \tag{31}$$

where

$$x = \frac{I}{R(1 + \xi)^{1/2}} \left(\frac{R}{r_1}\right)\left(\frac{p_a}{p}\right)^{s/2},$$

then Appendix B shows that

$$\sigma(\phi, p) = K_1 (\phi - \phi_1)^f \left(\frac{p}{p_a}\right)^s \tag{32}$$

and

$$u(\phi, p) = K_2 (\phi - \phi_1)^g \left(\frac{p}{p_a}\right)^t \tag{33}$$

where f, K_1, g, and K_2 are explicitly given in terms of n, C_1, m, and C_2, and vice versa.

At this point, we may turn the procedure around and fit the actual $\sigma(\phi, p_a)$ and $u(\phi, p_a)$ curves with the constants of the analytical expressions for $\sigma(\phi, p_a)$ and $u(\phi, p_a)$ (in the above example, ϕ_1, f, K_1, g, and K_2). This process in turn establishes the Ψ and Φ functions, and R/r_1 by Eq. (26).

Continuing with the example by fitting Eqs. (32) and (33) to argon and nitrogen (see Figs. 10, 11):

Argon		Nitrogen	
ϕ_1	= 500	ϕ_1	= 9000
f	= 1/3	f	= 1/3
K_1	= 292	K_1	= 210
g	= 1/2	g	= 2/3
K_2	= 3.60×10^7	K_2	= 2.30×10^6

The above values of the fitted constants may be used in turn in the equations of Appendix B to give values of (n, C_1, m, C_2), which, along with Eqs. (30) and (31), define the Ψ and Φ functions for use in Eqs. (24) and (25). Equation (26) for R/r_1 may then be used to relate the results to the experimental parameters (Eqs. (28) and (29)) and the "modified linear theory" may be plotted on Figs. 12, 13, 14, and 15.

The modified linear theory may be further reduced, yielding the ratio of power radiated to power conducted ξ, the electric field E, the arc current I, and the power radiated per unit length P_{rad}, as detailed in Appendix B. The results are plotted on Figs. 2 to 9.

In general, the proper trends with respect to current and pressure are exhibited, and the agreement may be said to be "good", particularly considering the simplicity and resulting ease of calculation of the expressions used.

6. CONCLUSIONS

In order to have a model describing both the "heating" and the "asymptotic" regions of a wall-stabilized arc column, a linearized analysis was made following Stine-Watson, but including radiation. Attempting to account for certain failings in the linear theory, the solutions were "modified" by allowing the slopes of the linear approximations to $\sigma(\phi)$ and $u(\phi)$ to vary with ϕ; the results (as applied to the asymptotic region, initially) are as follows:

1. The functional dependences of the various parameters are now approximately correct compared to the linear theory (particularly the electric field as a function of current).
2. The curve fitting of the plasma property curves $\sigma(\phi)$ and $u(\phi)$ using simple power laws is considerably more flexible and less arbitrary than the straight line approximations in the linear theory. The fact that $\sigma(\phi)$ and $u(\phi)$ shared a common constant parameter ϕ_1, did not seem to be too restrictive.
3. An "effective" arc-to-wall radius ratio, $\frac{r_1}{R}$, is defined which may be followed through the equations and studied in the solutions.
4. Similarity forms are suggested by the modified linear theory, or alternately through approximations to the basic equations; these are quite useful for plotting experimental results and collapsing theoretical calculations, and afford a direct comparison between the two.
5. For scaling and predicting purposes, the results are presented in alternate forms such that the best information, whether experimental or theoretical, may be used. (For example,

experimental curves at 1.0 atmosphere may be scaled as a function of pressure using theoretical powers of pressure, and analytical expressions).

6. There is strong evidence that the "deviations from experiment" of an exact solution using present "state of the art" calculations of plasma properties are at least as large as the deviations introduced by the approximations in the modified linear theory. The fact that functions are known for argon and nitrogen plasma properties that will reproduce the experimental results (at atmospheric pressures) in an exact calculation is beside the point because they were derived precisely with that constraint. Hence, in a practical sense, there is little value in using exact numerical calculations for arc column analysis, even for the prediction of absolute magnitudes. An interesting trend noted is that the modified linear theory and the AVCO[1] plasma properties seem to have their "errors" in opposite directions so that using approximations to the AVCO plasma properties in the modified linear theory gives better agreement than the "exact" calculations. The above chance effect was noted with nitrogen and with argon (using AVCO-type argon calculations) but might be expected to hold with other gases, since similar formulas and shapes of curves are involved.

Eventually the real value of such methods as the modified linear theory may be shown in the gas heating region by providing the insight needed to incorporate additional items (such as radiation and arc radius) into the simple theories.

Experiments in the gas heating region, including the measurement of radiation, are urgently needed for further comparisons.

APPENDIX A

DERIVATION OF THE ASYMPTOTIC REGION SIMILARITY RELATIONSHIPS FROM BASIC EQUATIONS

The well-known Elenbaas-Heller differential equation for an optically thin, steady state, axially symmetric arc of radius R and constant electric field strength E may be written in the following form (using Ohm's Law):

$$R^2 E^2 \sigma(\phi, p)\left[1 - \frac{u(\phi, p)}{\sigma(\phi, p) E^2}\right] = -\frac{1}{\rho}\frac{\partial}{\partial \rho}\left(\rho \frac{\partial \phi}{\partial \rho}\right) \qquad (1$$

$$\text{at } \rho = 0, \frac{\partial \phi}{\partial \rho} = 0$$

$$\text{at } \rho = 1, \phi = 0$$

In the above equation,

$$\rho = r/R$$

$$\phi = \int_{T_w}^{T} K(T, p)\, dT = \phi(\text{Gas}, I, p, R, \rho, T_w)$$

$$E = E(\text{Gas}, I, p, R, T_w)$$

and T_w is the wall temperature (≈ 0).

Assume:

i) The ratio of u to σ is a function of pressure only.

$$\frac{u(\phi, p)}{\sigma(\phi, p)} = F(p) \qquad (3$$

and

ii) The ratio of the volumetric radiated power to the volumetric input power is the same as the ratio of the power radiated per unit length to the power input per unit length.

$$\frac{u(\phi, p)}{\sigma(\phi, p) E^2} = \frac{F(p)}{E^2} \text{ (by i)} = \frac{P_{rad}}{EI} \tag{36}$$

Under the assumption inherent in Eq. (34),

$$EI = P_{rad} + P_{cond} \tag{37}$$

where P_{cond} is the power conducted to the wall per unit length. Then

$$\left[1 - \frac{u(\phi, p)}{\sigma(\phi, p) E^2}\right] = \left[1 - \frac{P_{rad}}{P_{rad} + P_{cond}}\right] = \frac{1}{1 + \xi} \tag{38}$$

where

$$\xi = \xi(\text{Gas}, I, p, R, T_w) \equiv \frac{P_{rad}}{EI - P_{rad}} = \frac{P_{rad}}{P_{cond}} .$$

Eq. (34) becomes

$$\sigma(\phi, p)\left[\frac{ER}{(1 + \xi)^{1/2}}\right]^2 = -\frac{1}{\rho}\frac{\partial}{\partial\rho}\left(\rho \frac{\partial\phi}{\partial\rho}\right) \tag{39}$$

The total current may be obtained from Ohm's Law

$$I = \int_0^R j\, 2\pi r\, dr = R^2 E \int_0^1 \sigma(\phi, p)\, 2\pi \rho d\rho \tag{40}$$

Dividing both sides by $R(1 + \xi)^{1/2}$, and considering

$$\sigma(\phi, p) = \sigma\left(\frac{ER}{(1 + \xi)^{1/2}}, p, \rho\right) \quad \text{from Eq. (39),}$$

the following form results:

$$\frac{I}{R(1 + \xi)^{1/2}} = fn\left(\frac{ER}{(1 + \xi)^{1/2}}, p\right) \tag{41}$$

Turning to the radiation now, from Eq. (36)

$$P_{rad} = \frac{I}{E} F(p)$$

$$= R^2 \frac{\frac{I}{R (1 + \xi)^{1/2}}}{\frac{ER}{(1 + \xi)^{1/2}}} F(p) \tag{42}$$

Using Eq. (41),

$$\frac{P_{rad}}{R^2 F (p)} = fn\left(\frac{ER}{(1 + \xi)^{1/2}}, p\right) \tag{43}$$

The pressure dependence in Eqs. (41) and (43) can be completely included in the similarity expressions if the following further assumptions are made:

iii) $$\sigma (\phi, p) = \sigma (\phi, p_a)\left(\frac{p}{p_a}\right)^s \tag{44}$$

and iv) $$u (\phi, p) = \left\langle\frac{u}{\sigma}\right\rangle_a \sigma(\phi, p_a)\left(\frac{p}{p_a}\right)^t \tag{45}$$

where p_a is a reference pressure (taken to be atmospheric for convenience), and $\left\langle\frac{u}{\sigma}\right\rangle_a = \frac{u (\phi, p_a)}{\sigma (\phi, p_a)}$ is some average value of $\left(\frac{u}{\sigma}\right)$ over the range of interest, evaluated at the reference pressure.

These further assumptions may be carried through the equations and the final results summarized as follows:

With $$\sigma (\phi, p) = \sigma (\phi, p_a)\left(\frac{p}{p_a}\right)^s \tag{46}$$

and $$\frac{u (\phi, p)}{\sigma (\phi, p) E^2} = \frac{\left\langle\frac{u}{\sigma}\right\rangle_a}{E^2}\left(\frac{p}{p_a}\right)^{t-s} = \frac{P_{rad}}{EI} \tag{47}$$

then

$$\frac{ER\left(\frac{p}{p_a}\right)^{s/2}}{(1+\xi)^{1/2}} = \psi'\left(\frac{I}{R(1+\xi)^{1/2}}\left(\frac{p_a}{p}\right)^{s/2}\right) \tag{48}$$

$$\frac{P_{rad}}{R^2}\left(\frac{p_a}{p}\right)^{t} = \phi'\left(\frac{I}{R\,(1+\xi)^{1/2}}\left(\frac{p_a}{p}\right)^{s/2}\right) \tag{49}$$

$$\xi = \frac{\left\langle\frac{u}{\sigma}\right\rangle_a\left(\frac{p}{p_a}\right)^{t} R^2}{\left[\psi'\left(\frac{I}{R\,(1+\xi)^{1/2}}\left(\frac{p_a}{p}\right)^{s/2}\right)\right]^2} \tag{50}$$

$$\left\langle\frac{u}{\sigma}\right\rangle_a = \left\langle\frac{u\,(\phi,\ p_a)}{\sigma\,(\phi,\ p_a)}\right\rangle \tag{51}$$

$$= \left\langle\frac{P_{rad}\ E}{I}\right\rangle_a \tag{52}$$

Of the quantities in the above equations, I, E, R, $(\frac{p}{p_a})$, P_{rad} and $\xi \equiv \frac{P_{rad}}{EI - P_{rad}}$ are all measurable and have definite values at each experimental operating point.

The quantities s and t are theoretical, or, alternately, fitted from experiments.

The quantity $\left\langle\frac{u}{\sigma}\right\rangle_a$ may be obtained either theoretically from Eq. (51), or experimentally from Fq. (52) by averaging experimental quantities over the region of interest at the reference pressure p_a.

An interesting check of the above similarity forms is provided by plotting the results of extensive arc column calculations using the above similarity variables; for example, the calculated "exact" nitrogen solutions of [1], which cover a very wide range of parameters, may be

so plotted.

First, the usual non-radiating similarity parameters ER vs I/R are plotted in Fig. 16. Each individual symbol represents one calculated condition obtained by assuming values for the electric field and axis temperature and then calculating the other parameters of interest (including wall radius). In general, calculations of this nature are difficult to compare directly with experiment because of the varying wall radius; however, if the similarity expressions hold, this variation will be of no consequence. The measurements of Maecker[4] are also dashed-in on Fig. 16 for reference. The effect of radiation in this plot is to scatter points upward from base lines of zero radiation at each pressure.

Next, the similarity parameters for constant pressure are plotted in Fig. 17. The use of these parameters very effectively collapses most of the points to the appropriate zero-radiation curve for each pressure.

Now an attempt will be made to further reduce the calculations by including pressure explicitly in the plotting parameters. Ref. 1 gives fitted expressions for σ, ϕ, and u which may be applied to nitrogen above 30,000 ^{o}K (See Eqs. (65), (67) and (73) of Ref. 1). From these equations, $\frac{u(\phi, p)}{\sigma(\phi, p)}$ is insensitive to ϕ (fulfilling assumption i), $s = 0.154$ and $t = 1.806$. Accordingly, Figs. 18 and 19 may be plotted. As expected, the pressure dependence over-compensated at the low temperature end of Fig. 18 but in general did a remarkable job of collapsing the data in the two figures. Particularly satisfying in Fig. 19 was the manner in which (compared to a $\frac{P_{rad}}{R^2}$ vs $\frac{I}{R}$ plot) the ξ parameter adjusted the points at each pressure to fall on continuous similar curves, the $\left(\frac{p_a}{p}\right)^{s/2}$ parameter moved the (similar) curves at the higher pressures to the left, and the $\left(\frac{p_a}{p}\right)^{t}$ parameter collapsed the curves downwards to the atmospheric pressure curve. Figs. 17, 18 and 19 also indicate

that s and t values can probably be assigned such that the complete similarity forms may be used, at least piecewise, over the complete region of interest.

Finally, a direct comparison may now be made between the calculations[1] and the experiments of Maecker[4] for nitrogen with no problems involving different operating conditions confusing the results. The disagreements shown on Figs. 17, 18, 19, or Figs. 13, 15 occur essentially because the AVCO[1] electrical conductivity is as much as 60% higher and the volumetric radiated power as much as a factor of 5 higher than the equivalent properties obtained from the inversion of Maecker's measurements in[7].

APPENDIX B

THE MODIFIED LINEAR THEORY SOLUTION

From the exact linear solution, Eqs. (17), (18), and (12) combined with Eq. (11), may be written as follows:

$$\frac{ER\left(\frac{r_1}{R}\right)\left(\frac{p}{p_a}\right)^{s/2}}{(1+\xi)^{1/2}} = \frac{2.4}{\left\langle\frac{d\sigma}{d\phi}\right\rangle_a^{1/2}} \tag{53}$$

$$\frac{I\left(\frac{R}{r_1}\right)\left(\frac{p_a}{p}\right)^{s/2}}{R\,(1+\xi)^{1/2}} = 2\pi\, J_1\,(2.4)\left\langle\frac{d\sigma}{d\phi}\right\rangle_a^{1/2}(\phi_{axis} - \phi_1) \tag{54}$$

$$\frac{P_{rad}}{R^2}\left(\frac{R}{r_1}\right)^2\left(\frac{p_a}{p}\right)^t = \frac{\left\langle\frac{du}{d\phi}\right\rangle_a}{2.4\left\langle\frac{d\sigma}{d\phi}\right\rangle_a^{1/2}}\,\frac{I\left(\frac{R}{r_1}\right)\left(\frac{p_a}{p}\right)^{s/2}}{R\,(1+\xi)^{1/2}} \tag{55}$$

The linear theory becomes "modified" by allowing $\left\langle\frac{d\sigma}{d\phi}\right\rangle_a$ and $\left\langle\frac{du}{d\phi}\right\rangle_a$, the "average" slopes of $\sigma(\phi, p_a)$ and $u(\phi, p_a)$ respectively, to become functions of $(\phi-\phi_1)$ in the solution.

Considering $\left\langle\frac{d\sigma}{d\phi}\right\rangle_a$ and $\left\langle\frac{du}{d\phi}\right\rangle_a$ to be functions of $(\phi-\phi_1)$, then from Eqs. (53), (54), and (55)

$$\frac{ER\left(\frac{r_1}{R}\right)\left(\frac{p}{p_a}\right)^{s/2}}{(1+\xi)^{1/2}} = \Psi\,\frac{I\left(\frac{R}{r_1}\right)\left(\frac{p_a}{p}\right)^{s/2}}{R\,(1+\xi)^{1/2}} \tag{56}$$

and

$$\frac{P_{rad}}{R^2}\left(\frac{R}{r_1}\right)^2\left(\frac{p_a}{p}\right)^t = \Phi\left(\frac{I\left(\frac{R}{r_1}\right)\left(\frac{p_a}{p}\right)^{s/2}}{R\,(1+\xi)^{1/2}}\right) \tag{57}$$

To simplify, assume the following forms for Ψ and Φ:

$$\Psi(x) = C_1 x^n \tag{58}$$

$$\Phi(x) = C_2 x^m \tag{59}$$

where

$$x = \frac{I}{R\,(1+\xi)^{1/2}}\left(\frac{R}{r_1}\right)\left(\frac{p_a}{p}\right)^{s/2}$$

Then, from Eqs. (53), (56), and (58),

$$\left\langle\frac{d\sigma}{d\phi}\right\rangle_a^{1/2} = \frac{2.4}{C_1}x^{-n}$$

$$= \frac{2.4}{C_1\left[2\pi J_1(2.4)\right]^n\left\langle\frac{d\sigma}{d\phi}\right\rangle_a^{n/2}(\phi-\phi_1)^n} \quad \text{(from Eq. 54)}$$

Solving for $\left\langle\frac{d\sigma}{d\phi}\right\rangle_a$,

$$\left\langle\frac{d\sigma}{d\phi}\right\rangle_a = \frac{\left(\frac{2.4}{C_1}\right)^{\frac{2}{n+1}}}{\left[2\pi J_1(2.4)\right]^{\frac{2n}{n+1}}}(\phi-\phi_1)^{\frac{-2n}{n+1}} \tag{60}$$

Also, from Eqs. (55), (57), and (59),

$$\left\langle \frac{du}{d\phi} \right\rangle_a = C_2 \, x^{m-1} \, (2.4) \left\langle \frac{d\sigma}{d\phi} \right\rangle_a^{1/2}$$

$$= 2.4 \, C_2 \left[2\pi \, J_1(2.4) \left\langle \frac{d\sigma}{d\phi} \right\rangle_a^{1/2} (\phi - \phi_1) \right]^{m-1} \left\langle \frac{d\sigma}{d\phi} \right\rangle_a^{1/2} \text{ (from Eq. 54)}$$

Substituting for $\left\langle \frac{d\sigma}{d\phi} \right\rangle_a$,

$$\left\langle \frac{du}{d\phi} \right\rangle_a = 2.4 \, C_2 \left(\frac{2.4}{C_1} \right)^{\frac{m}{n+1}} \left[2\pi \, J_1(2.4) \right]^{\frac{m-n-1}{n+1}} (\phi - \phi_1)^{\frac{m-n-1}{n+1}} \tag{61}$$

Finally, σ may be evaluated in terms of ϕ:

$$\sigma(\phi, \, p_a) = \left\langle \frac{d\sigma}{d\phi} \right\rangle_a (\phi - \phi_1) = \frac{\left(\frac{2.4}{C_1} \right)^{\frac{2}{n+1}}}{\left[2\pi \, J_1 \, (2.4) \right]^{\frac{2n}{n+1}}} (\phi - \phi_1)^{\frac{1-n}{1+n}} \tag{62}$$

$$= K_1 \, (\phi - \phi_1)^f \tag{63}$$

where

$$f = \frac{1-n}{1+n} \tag{64}$$

$$K_1 = \frac{\left(\frac{2.4}{C_1} \right)^{\frac{2}{n+1}}}{\left[2\pi \, J_1(2.4) \right]^{\frac{2n}{n+1}}} \tag{65}$$

or

$$n = \frac{1-f}{1+f} \tag{66}$$

$$C_1 = \frac{2.4}{K_1 \frac{1}{1+f} \left[2\pi J_1(2.4)\right]^{\frac{1-f}{1+f}}} \tag{67}$$

Similarly, u may be evaluated in terms of ϕ:

$$u(\phi, p_a) = \left\langle \frac{du}{d\phi} \right\rangle_a (\phi-\phi_1) = 2.4\, C_2 \left(\frac{2.4}{C_1}\right)^{\frac{m}{n+1}} \left[2\pi J_1(2.4)\right]^{\left(\frac{m-n-1}{n+1}\right)} (\phi-\phi_1)^{\frac{m}{n-1}} \tag{68}$$

$$\equiv K_2 (\phi-\phi_1)^g \tag{69}$$

where

$$g = \frac{m}{n+1} \tag{70}$$

$$K_2 = 2.4\, C_2 \left(\frac{2.4}{C_1}\right)^{\frac{m}{n+1}} \left[2\pi J_1 (2.4)\right]^{\left(\frac{m-n-1}{n+1}\right)} \tag{71}$$

or

$$m = \frac{2g}{1+f} \tag{72}$$

$$C_2 = \frac{K_2}{2.4} \frac{1}{K_1 \frac{g}{1+f} \left[2\pi J_1 (2.4)\right]^{\left(\frac{2g-f-1}{1+f}\right)}} \tag{73}$$

Hence, if the group of parameters (n, C_1, m, C_2) is known, the group (f, K_1, g, K_2) may be calculated from Eqs. (64), (65), (70), and (71). Conversely, if the group (f, K_1, g, K_2) is known (for example, by curve fitting $\sigma(\phi, p_a)$ and $u(\phi, p_a)$, the group (n, C_1, m, C_2) may be calculated from Eqs. (66), (67), (72), and (73).

For example, assume that the experimental results can be plotted using the following similarity forms (including fitting values of s and t, if needed):

$$\frac{ER}{(1+\xi)^{1/2}}\left(\frac{p}{p_a}\right)^{s/2} = \Psi'\left(\frac{I\left(\frac{p_a}{p}\right)^{s/2}}{R\,(1+\xi)^{1/2}}\right) \tag{74}$$

$$\frac{P_{rad}}{R^2}\left(\frac{p_a}{p}\right)^{t} = \Phi'\left(\frac{I\left(\frac{p_a}{p}\right)^{s/2}}{R\,(1+\xi)^{1/2}}\right) \tag{75}$$

If a reasonable value of ϕ_1 can be assigned (say from fitting theoretical curves of $\sigma(\phi, p_a)$ and $u(\phi, p_a)$ near the axis), then from Eqs. (26) and (74)

$$\frac{R}{r_1} = \exp\left\{\frac{2\pi\,\phi_1}{\Psi'\left(\frac{I\left(\frac{p_a}{p}\right)^{s/2}}{R\,(1+\xi)^{1/2}}\right)\cdot\frac{I\left(\frac{p_a}{p}\right)^{s/2}}{R\,(1+\xi)^{1/2}}}\right\} \tag{76}$$

and the similarity forms in Eqs. (56) and (57) may be plotted. These plots may be fitted with (n, C_1, m, C_2) from Eqs. (58) and (59) and thus (f, K_1, g, K_2) may be calculated. The shapes of the $\sigma(\phi, p)$ and $u(\phi, p)$ curves implied by the experimental results are then given by:

$$\sigma(\phi,\ p) = K_1\ (\phi-\phi_1)^f \left(\frac{p}{p_a}\right)^s \tag{77}$$

$$u(\phi,\ p) = K_2\ (\phi-\phi_1)^g \left(\frac{p}{p_a}\right)^t \tag{78}$$

Conversely, the similarity functions of Eqs. (74) and (75) may be obtained from the fitted shapes of the $\sigma(\phi,\ p_a)$ and $u(\phi,\ p_a)$ curves (yielding ϕ_1, f, K_1, g, K_2). After (n, C_1, m, C_2) is calculated, then $\frac{R}{r_1}$ may be calculated as a function of x from the following equation (see Eqs. (26), (56), and (58)):

$$\frac{R}{r_1} = \exp\left\{\frac{2\pi\ \phi_1}{C_1\ x^{n+1}}\right\} \tag{79}$$

where

$$x = \frac{I}{R\ (1 + \xi)^{1/2}} \left(\frac{R}{r_1}\right)\left(\frac{p_a}{p}\right)^{s/2}$$

Knowing $\frac{R}{r_1} = \frac{R}{r_1}(x)$, then the similarity functions of Eqs. (74) and (75) immediately follow using Eqs. (58) and (59).

If it is desired to obtain such quantities as electric field, current and radiated power per unit length for a specific geometry, an expression is needed for ξ from the modified theory.

The original expression for ξ was the following: (See Eq. 11)

$$\xi = \frac{R^2}{\left(\frac{R}{r_1}\right)^2}\ \frac{1}{(2.4)^2} \left\langle\frac{du}{d\phi}\right\rangle_a \left(\frac{p}{p_a}\right)^t.$$

From equations of the modified linear theory, with

$$\left(\frac{du}{d\phi}\right)_a = C_2 \, x^{m-1} \quad (2.4) \quad \left(\frac{d\sigma}{d\phi}\right)_a^{1/2}$$

and

$$\left(\frac{d\sigma}{d\phi}\right)_a^{1/2} \qquad \frac{2.4}{C_1} \, x^{-n},$$

then

$$\xi = \frac{R^2}{\left(\frac{R}{r_1}\right)^2} \left(\frac{p}{p_a}\right)^t \frac{C_2}{C_1} \, x^{m-n-1} = \xi\left(R, \left(\frac{p}{p_a}\right), x\right) \qquad (80$$

Hence after values of s and t are determined in addition to (ϕ_1, f, K_1, g and K_2) by curve fitting $\sigma(\phi, p)$ and $u(\phi, p)$ with the expressions of Eqs. (77) and (78), all quantities of interest may be obtained as a function of x for given values of R and $\left(\frac{p}{p_a}\right)$.

If constant current calculations are desired, simple cross plotting is necessary (as with the linear theory).

Accordingly, values of ξ have been calculated as functions of current and pressure for argon and nitrogen. The results are plotted in Figs. 20 to 23 along with experimental values and the predictions of the straight linear theory. The relationships between the modified linear theory and the experiments are what one would expect after examining the curve fits on Fig. 11. Figs. 20 to 23 may be used in turn to reduce the similarity form of the modified linear theory given on Figs. 12 to 15 back to the quantities plotted in Figs. 2 to 9 for a specific geometry. The results are discussed in Section 5.

The natural question arises as to the relation between the expression for ξ given by Eq. (80) and that given by Eq. (50) in

Appendix A, which was derived using assumptions in the basic equations.

Applying the assumptions of Appendix A to the present theory,

$$f = g \tag{81}$$

and

$$\left\langle \frac{u}{\sigma_a} \right\rangle = \frac{K_2}{K_1} \tag{82}$$

From Eqs. (64) and (70), then

$$m = 1 - n. \tag{83}$$

Hence

$$\xi = \frac{R^2}{\left(\frac{R}{r_1}\right)^2} \left(\frac{p}{p_a}\right)^t \frac{C_2}{C_1} \frac{1}{x^{2n}},$$

or

$$\xi = \frac{C_1 C_2 \left(\frac{p}{p_a}\right)^t R^2}{\left[\frac{R}{r_1} C_1 x^n\right]^2} \tag{84}$$

From Eqs. (67) and (73),

$$C_1 C_2 \frac{K_2}{K_1} = \left\langle \frac{u}{\sigma_a} \right\rangle \quad \text{(from Eq. 82).}$$

After replacing $\frac{R}{r_1} C_1 x^n$ with $\frac{ER\left(\frac{p}{p_a}\right)^{s/2}}{(1+\xi)^{1/2}}$ from the present theory,

Eq. (84) becomes identical with Eq. (50) combined with Eq. (48) of Appendix A.

Hence the modified linear theory reduces to the results given in Appendix A when $\sigma(\phi, p)$ and $u(\phi, p)$ are required to have the same ϕ dependence.

REFERENCES

1. AVCO-Rad Staff, "Theoretical and Experimental Investigation of Arc Plasma Generation Technology," ASD-TDR-62-729, Part II, Vol. 2, September 1963

2. L. Spitzer, Jr., Physics of Fully Ionized Gases, Interscience Publishers Inc., New York, 1956

3. A. Unsold, Physik der Sternatmospharen, 2nd ed., Springer, Berlin, 163-174 (1955)

4. H. Maecker, "Messung und Answertung von Bogencharakteristiken (Ar, N_2)," Zeitschrift fur Physik 158, 392-404 (1960)

5. G. Marlotte, "Basic Research on Gas Flows Through Electric Arcs, Phase II," Electro-Optical Systems, Inc., Interim Report under Contract AF 33(657)-7940, EOS 2181-IR-3, 11 March 1964

6. H. A. Stine and V. R. Watson, "The Theoretical Enthalpy Distribution of Air in Steady State Flow Along the Axis of a Direct Current Electric Arc," NASA TN-D-1331, August 1962

7. J. Uhlenbusch, Plasma Properties for (Ar, N_2) Obtained from the Measurements of Maecker (Ref. 4) (to be published)

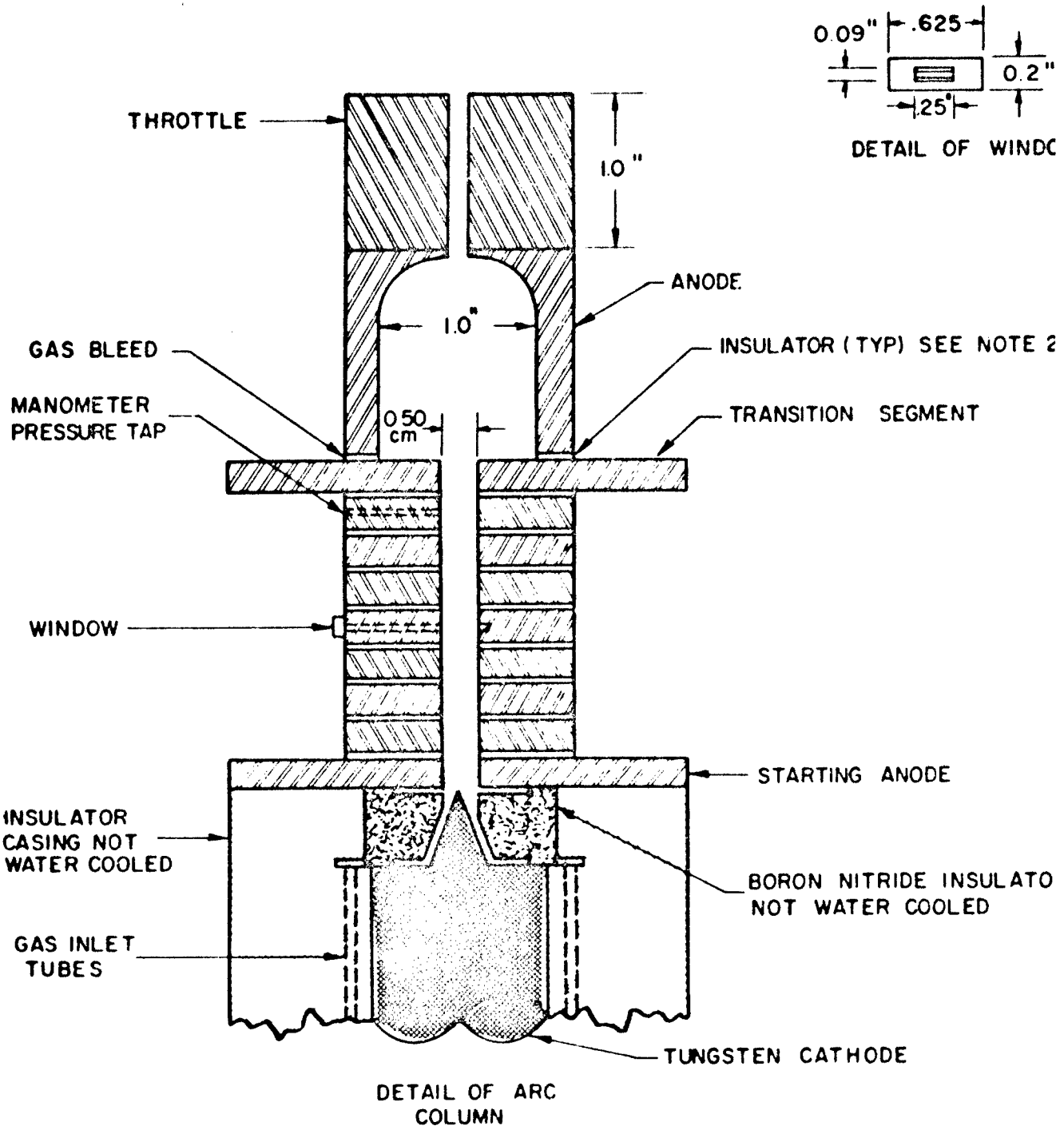

NOTE:

1. ALL COMPONENTS WATER COOLED UNLESS OTHERWISE NOTED
2. ALL INSULATORS BETWEEN COMPONENTS ARE A COMPOSITE OF BORON NITRIDE, TRANSITE & SILICON RUBBER

FIG. 1 ARC COLUMN SCHEMATIC

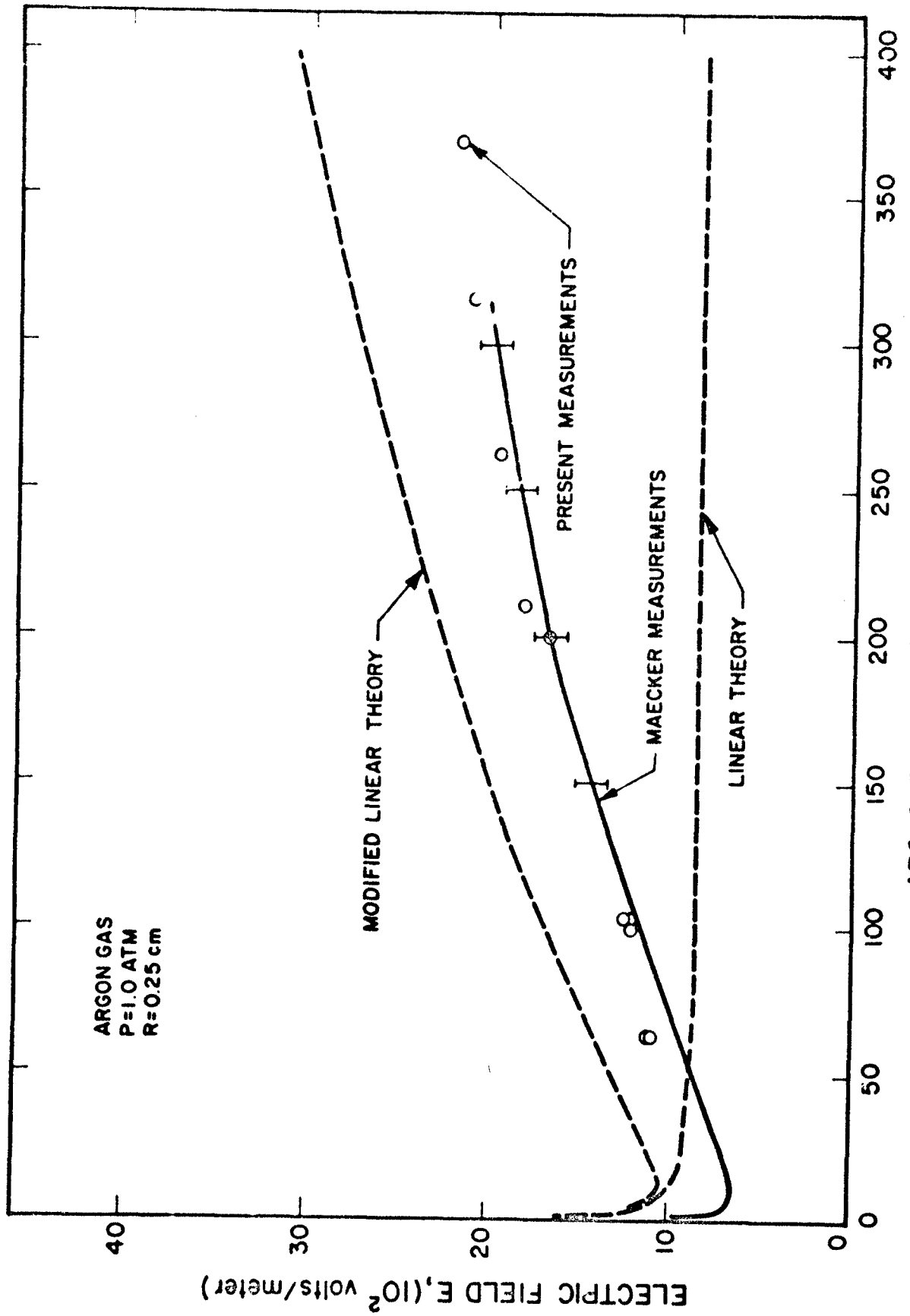

FIG. 2 ELECTRIC FIELD AS A FUNCTION OF CURRENT - ARGON GAS

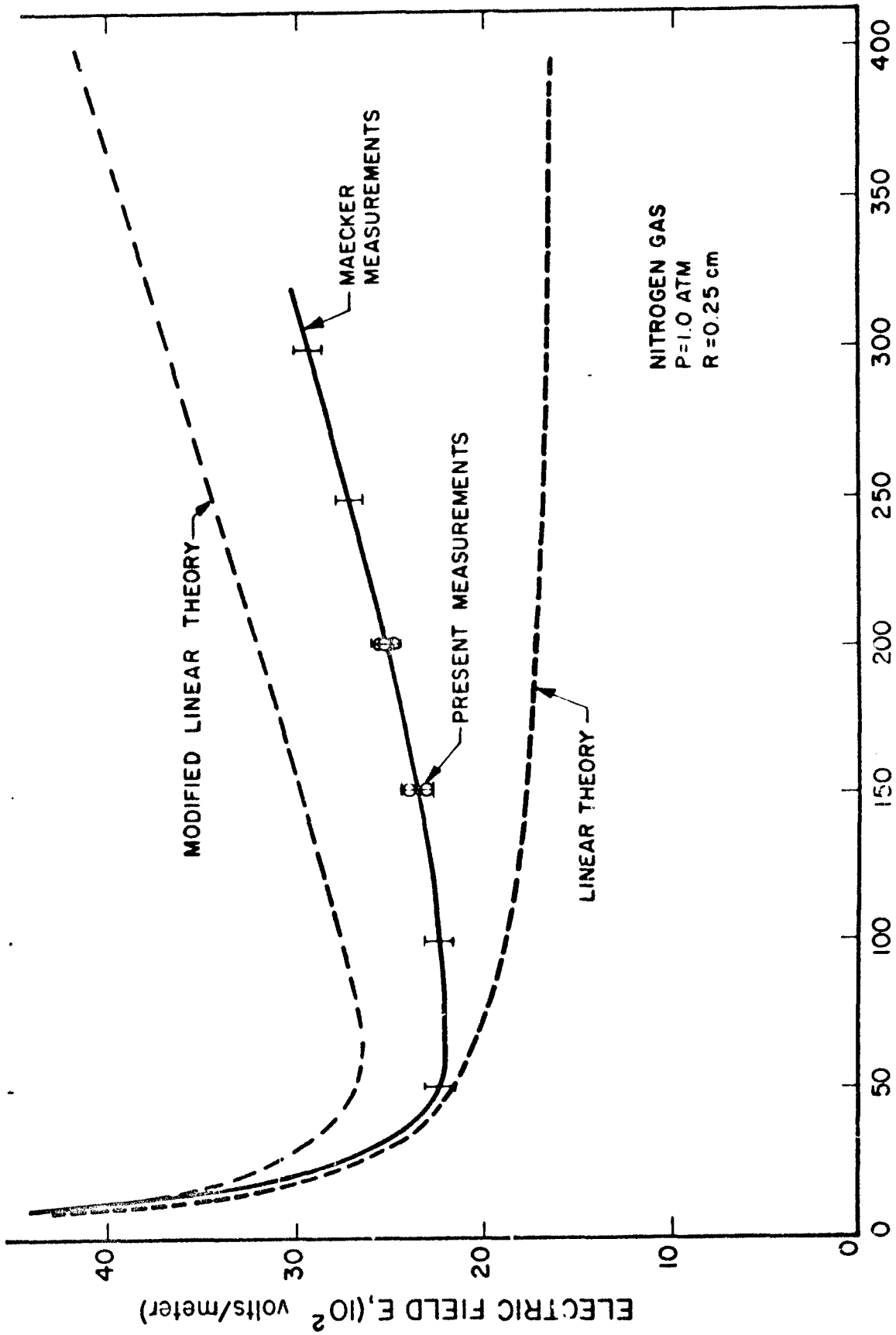

FIG. 3 ELECTRIC FIELD AS A FUNCTION OF CURRENT - NITROGEN GAS

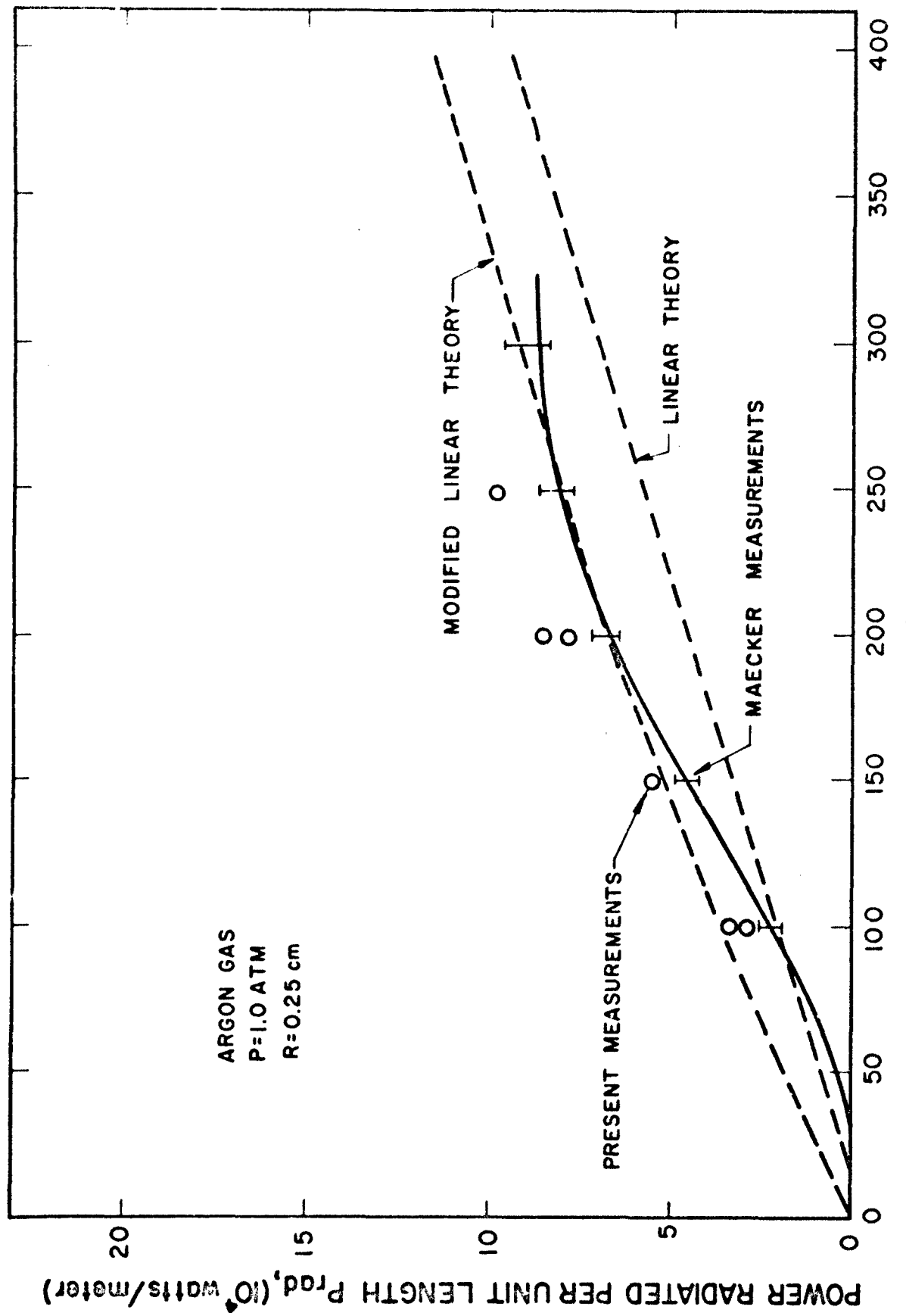

FIG. 4 POWER RADIATED PER UNIT LENGTH AS A FUNCTION OF CURRENT - ARGON GAS

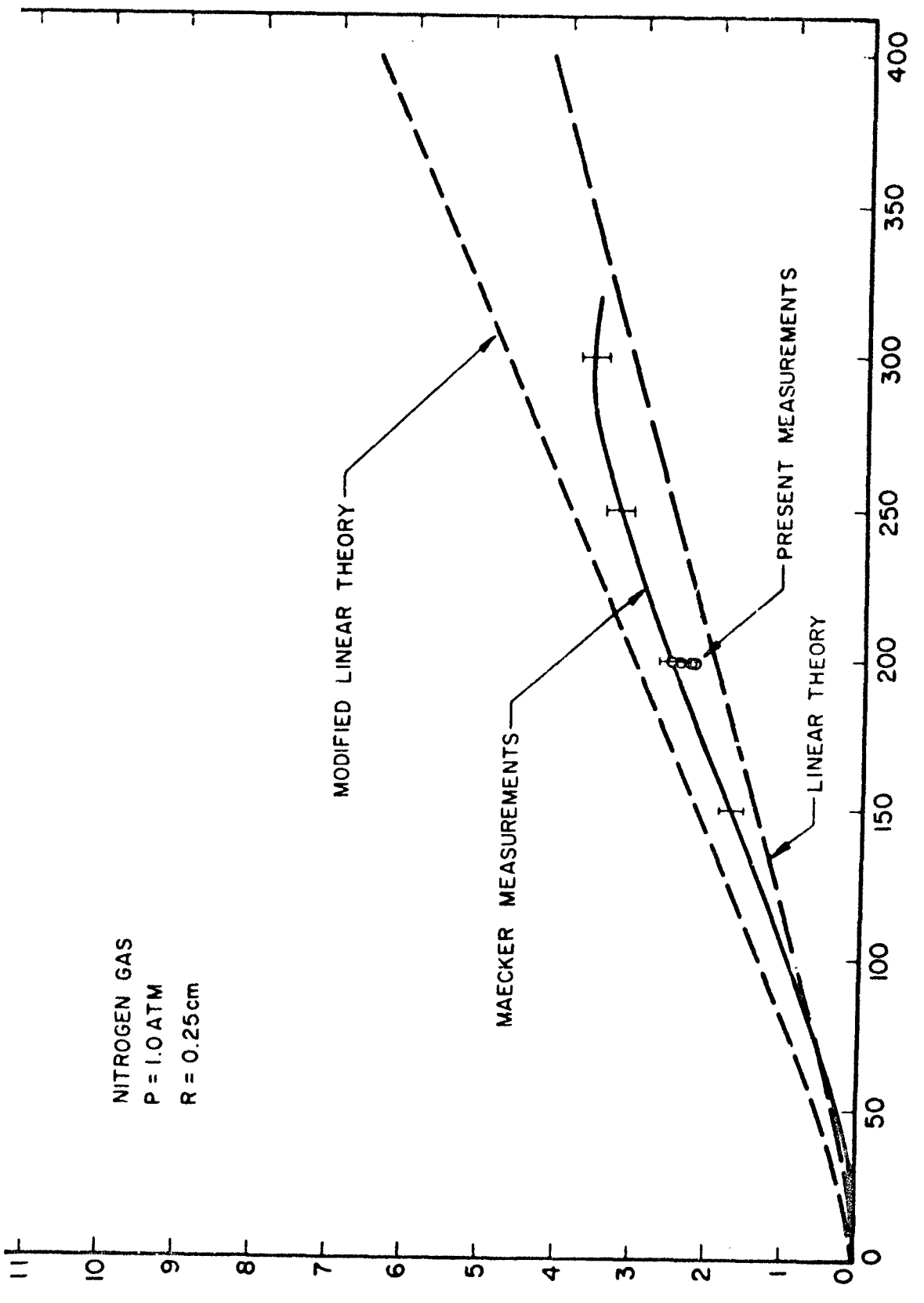

FIG. 5 POWER RADIATED PER UNIT LENGTH AS A FUNCTION OF CURRENT - NITROGEN GAS

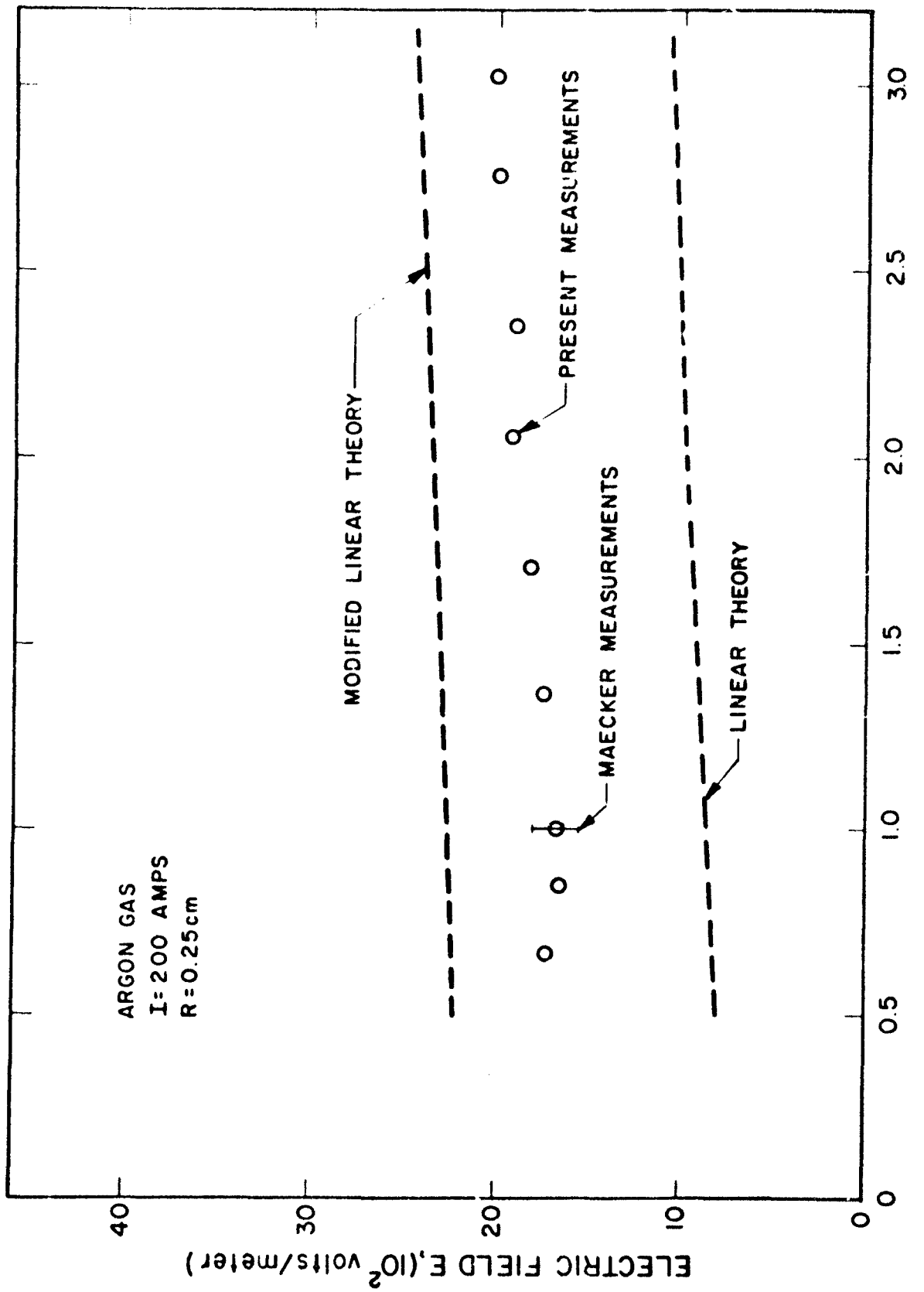

FIG. 6 ELECTRIC FIELD AS A FUNCTION OF PRESSURE - ARGON GAS

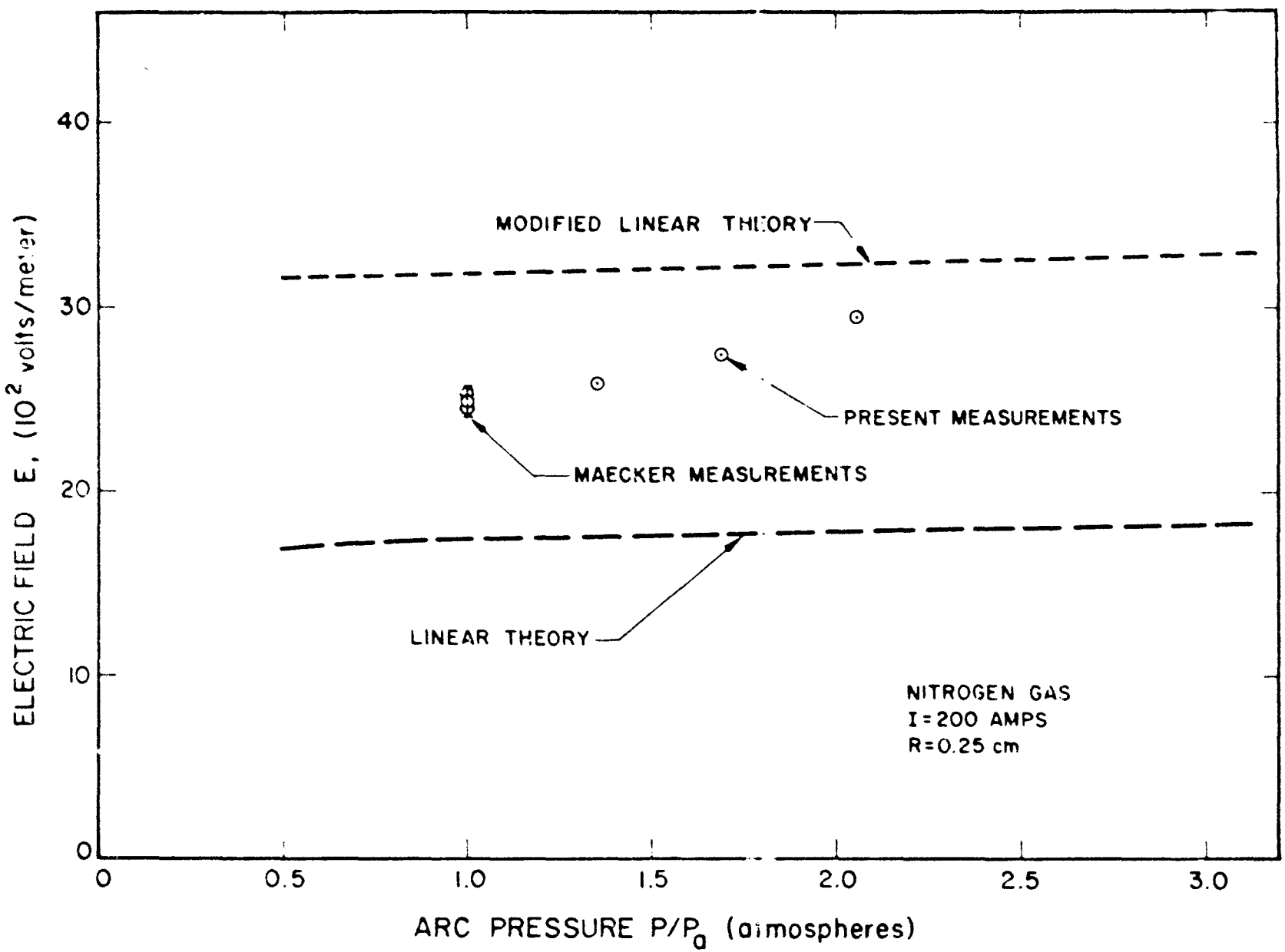

FIG. 7 ELECTRIC FIELD AS A FUNCTION OF PRESSURE - NITROGEN GAS

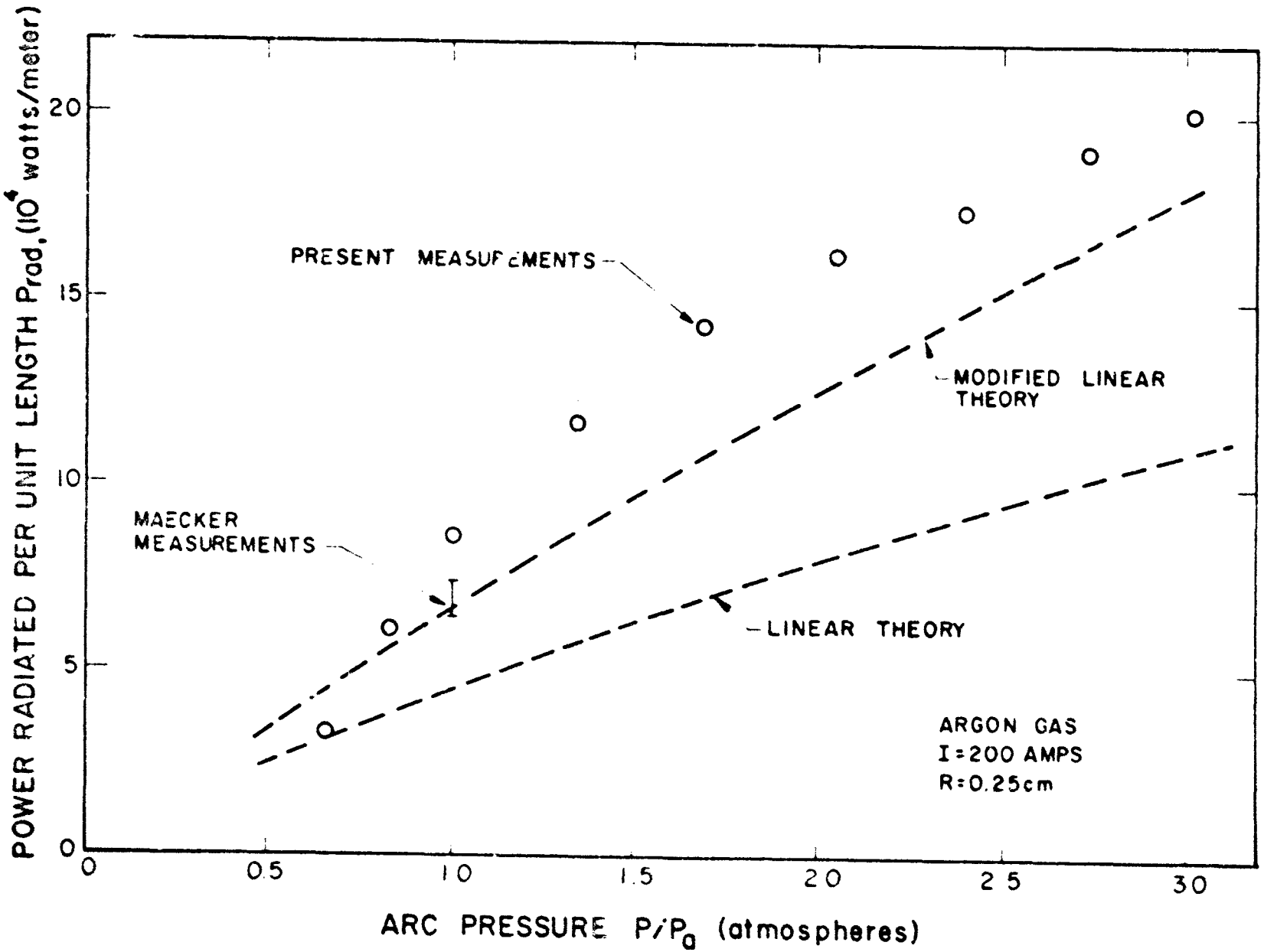

FIG. 8 POWER RADIATED PER UNIT LENGTH AS A FUNCTION OF PRESSURE - ARGON GAS

THIS

PAGE

IS

MISSING

IN

ORIGINAL

DOCUMENT

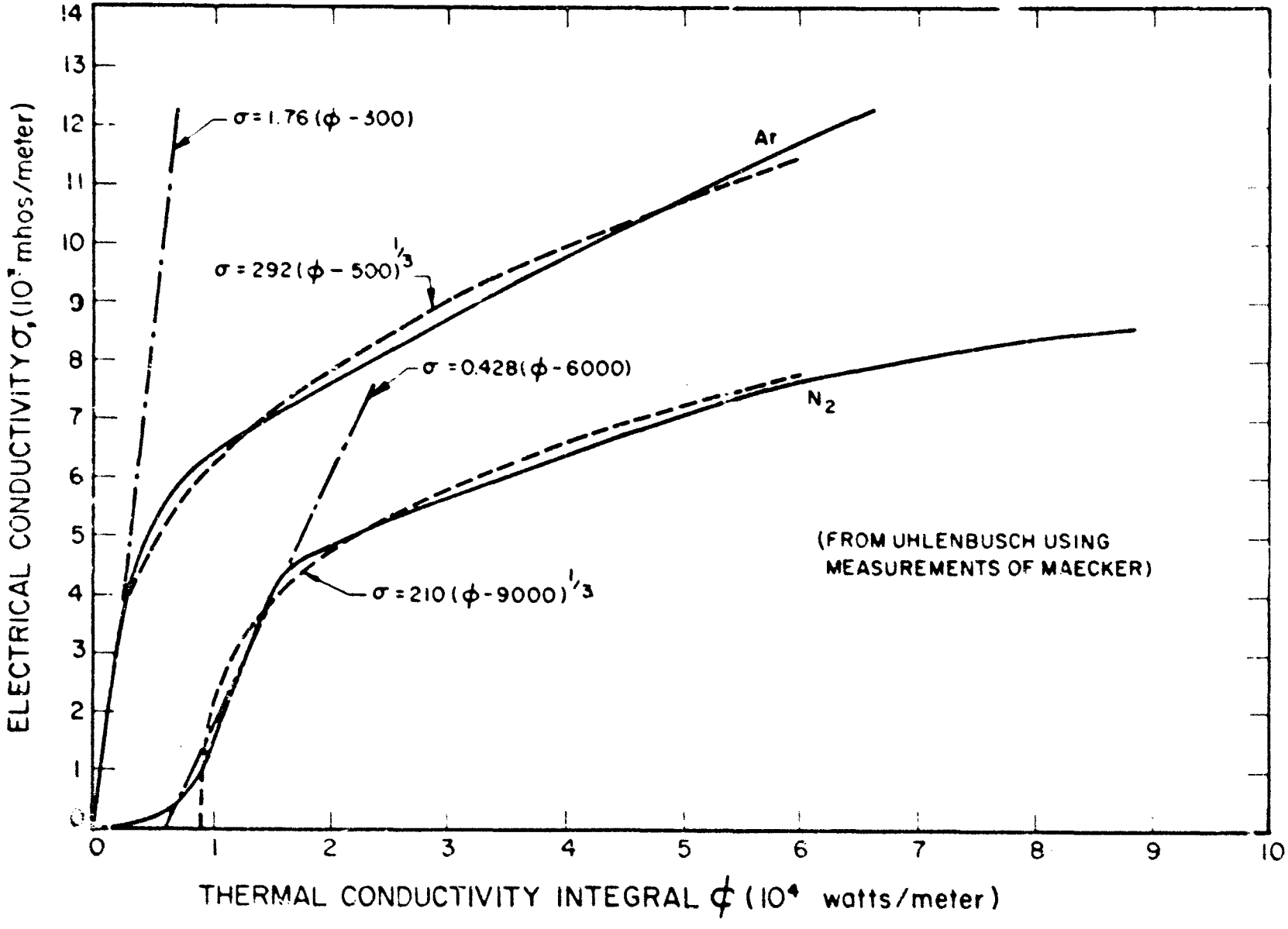

FIC. 10 ELECTRICAL CONDUCTIVITY AS A FUNCTION OF TH THERMAL CONDUCTIVITY INTEGRAL FOR ARGON

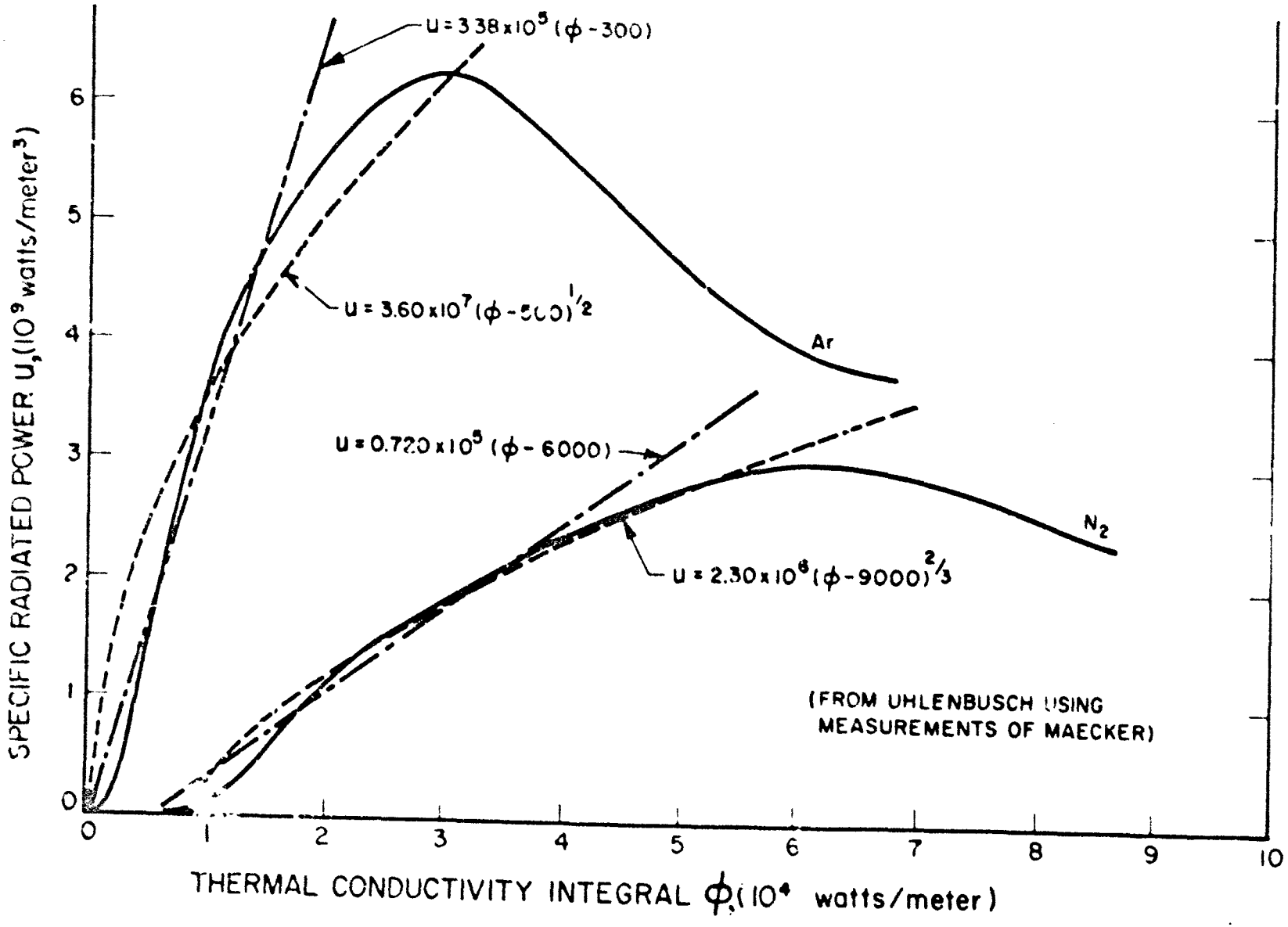

FIG. 11 SPECIFIC RADIATED POWER AS A FUNCTION OF THE THERMAL CONDUCTIVITY INTEGRAL FOR ARGON AND NITROGEN AT ATMOSPHERIC PRESSURE

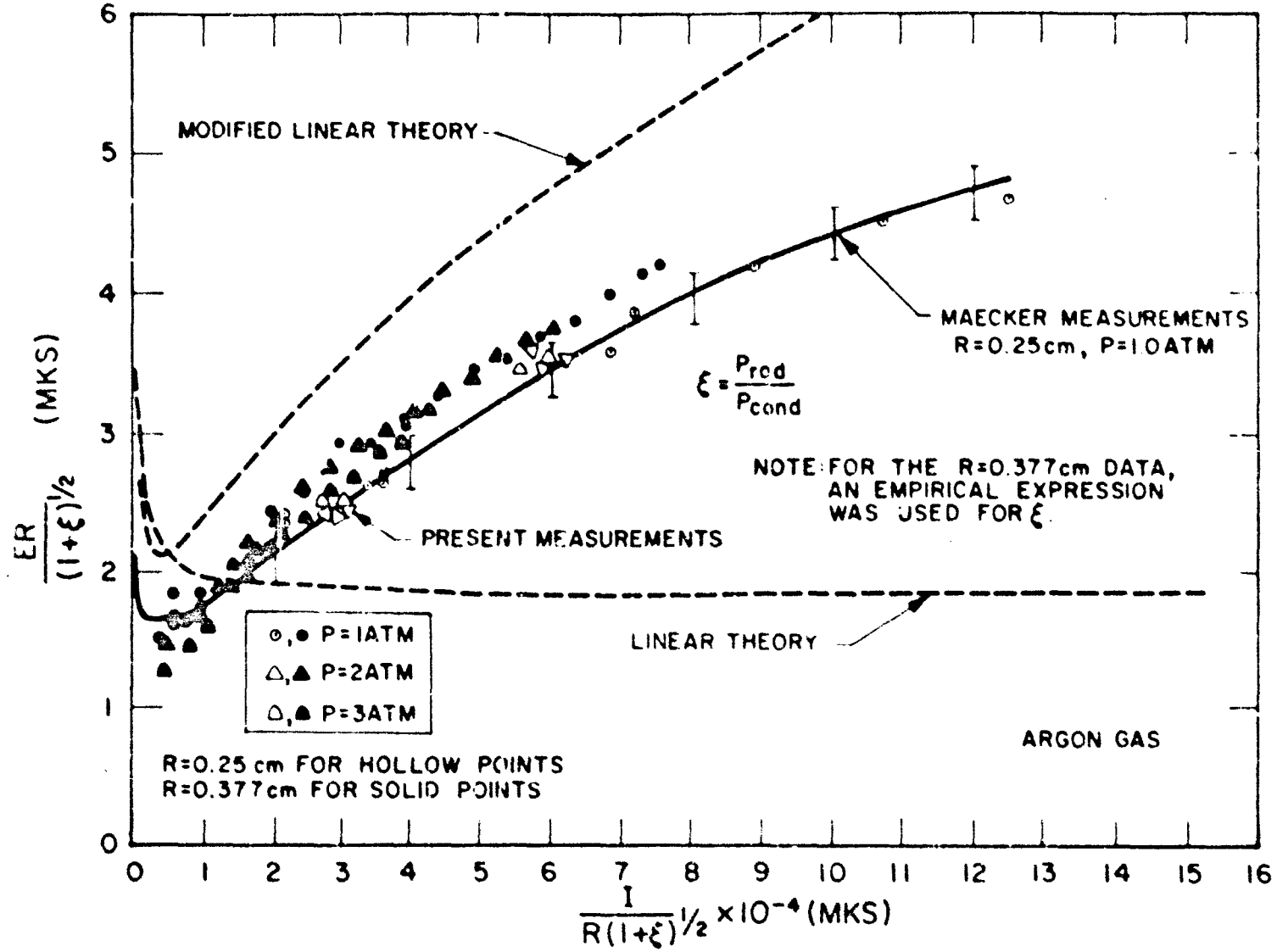

FIG. 12 ARC CHARACTERISTIC VALUES PLOTTED USING SIMILARITY VARIABLES - ARGON GAS

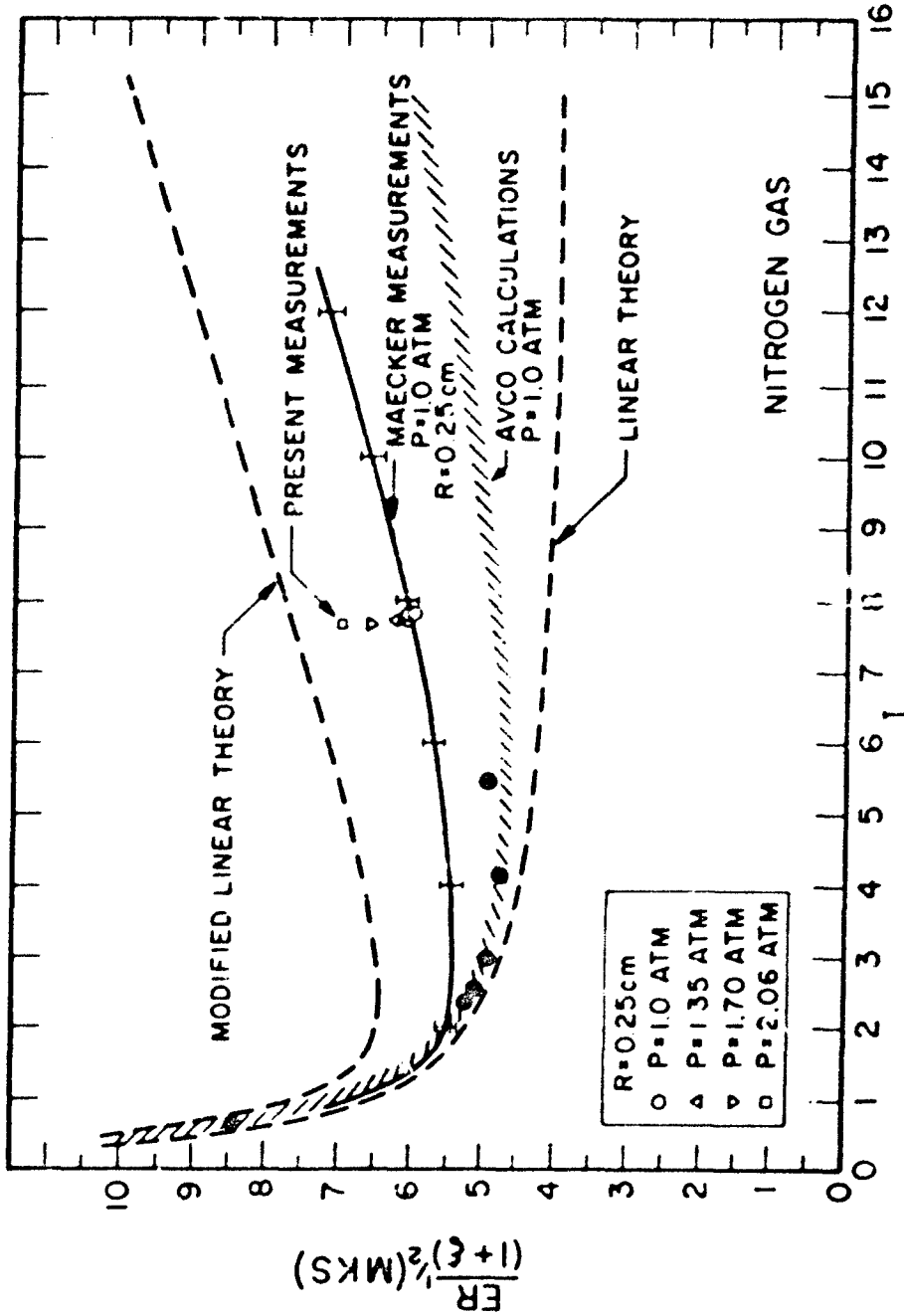

FIG. 13 ARC CHARACTERISTIC VALUES PLOTTED USING SIMILARITY VARIABLES - NITROGEN GAS

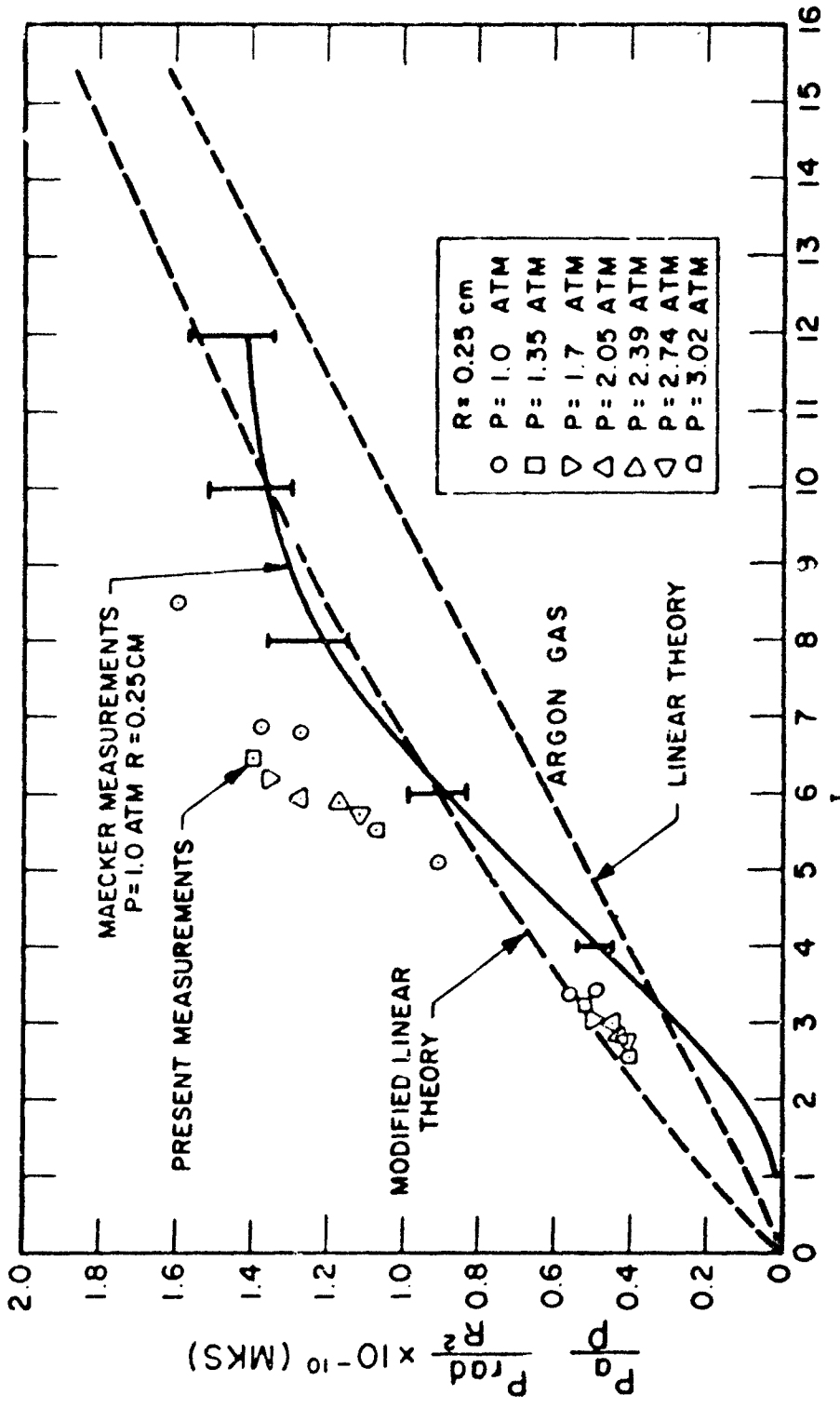

FIG. 14 RADIATED POWER PER UNIT LENGTH PLOTTED USING SIMILARITY VARIABLES - ARGON GAS

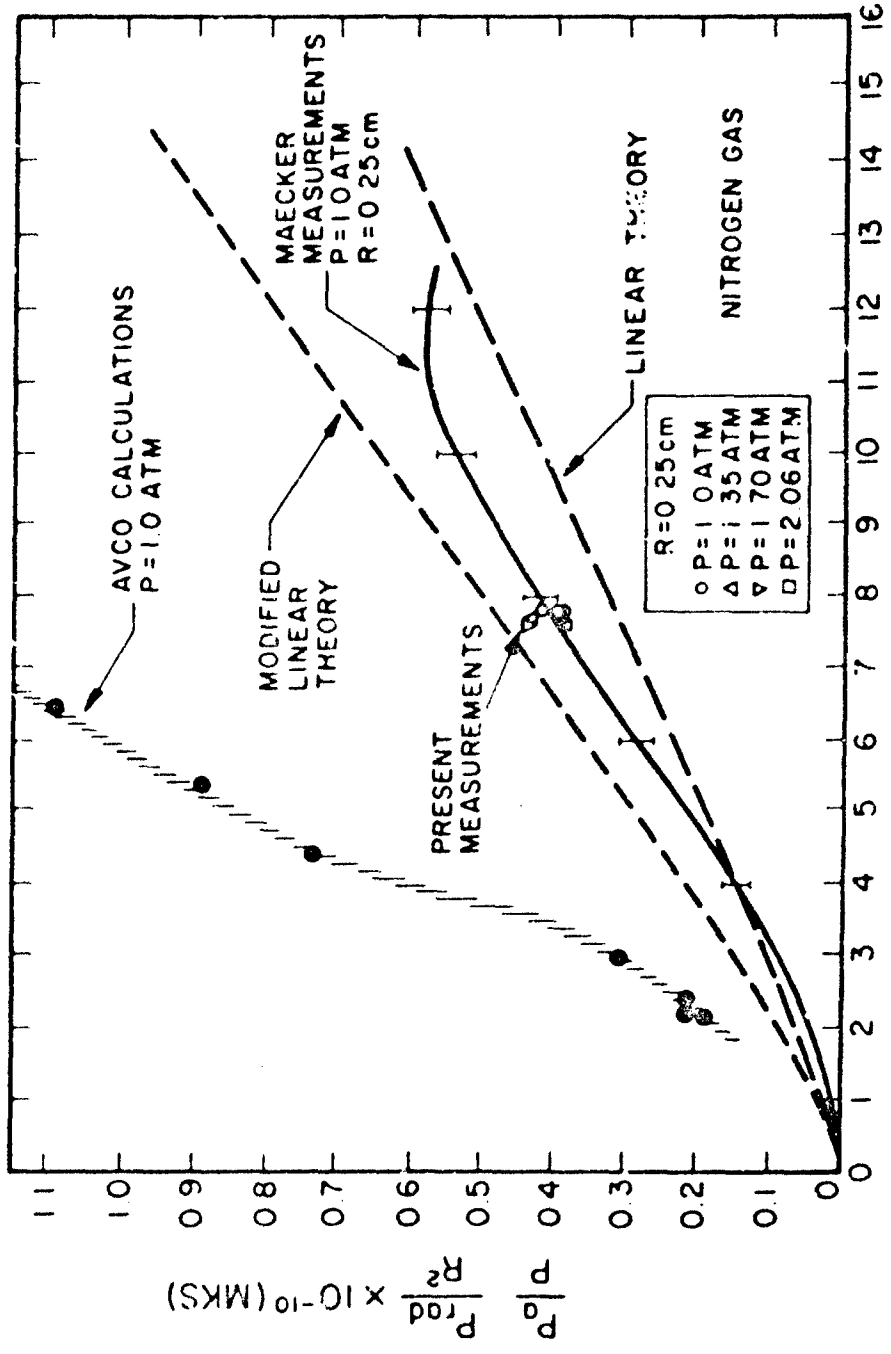

FIG. 15 RADIATED POWER PER UNIT LENGTH PLOTTED USING SIMILARITY VARIABLES - NITROGEN GAS

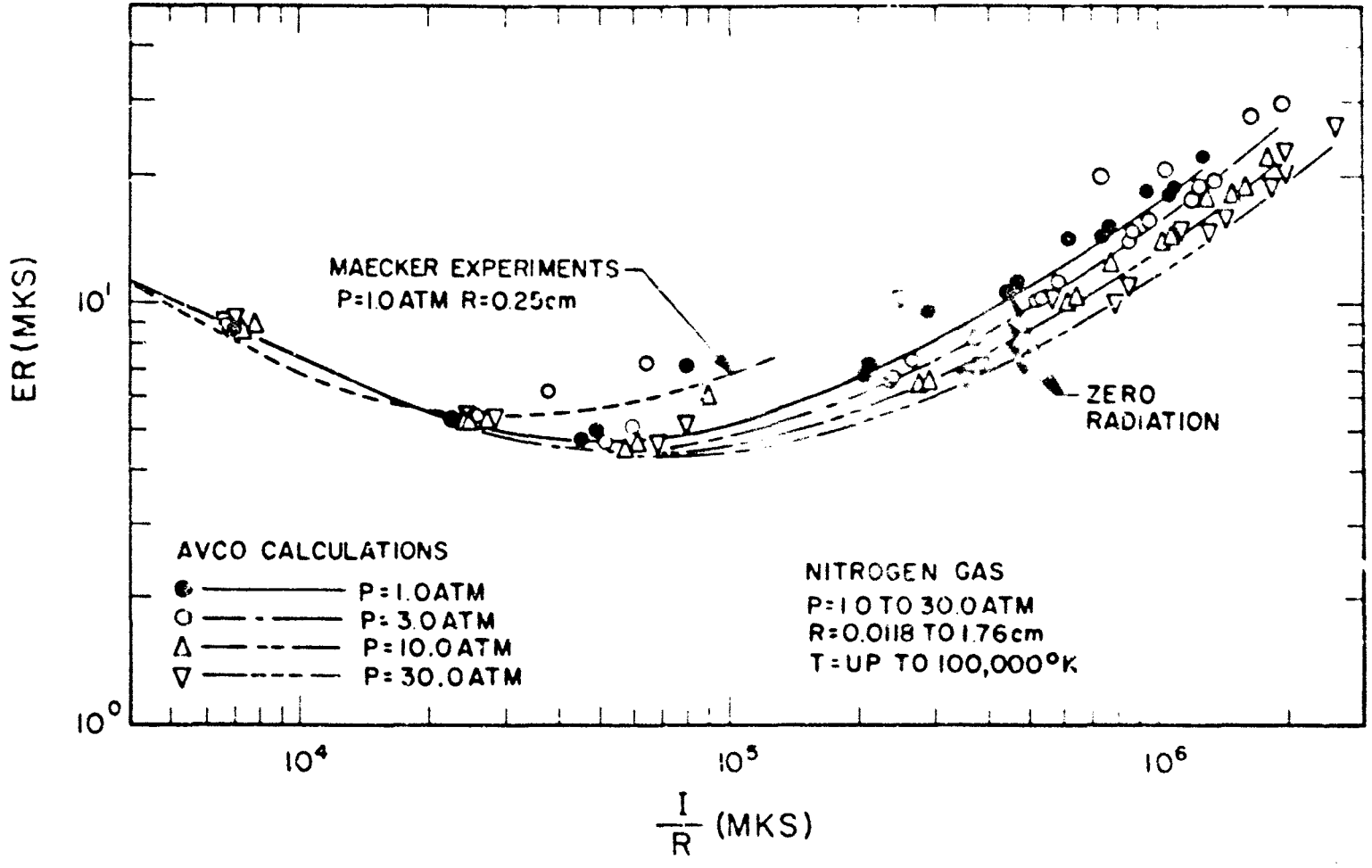

FIG. 16 CALCULATED NITROGEN CHARACTERISTICS PLOTTED WITH (N[illegible]ATING) SIMILARITY VARIABLES

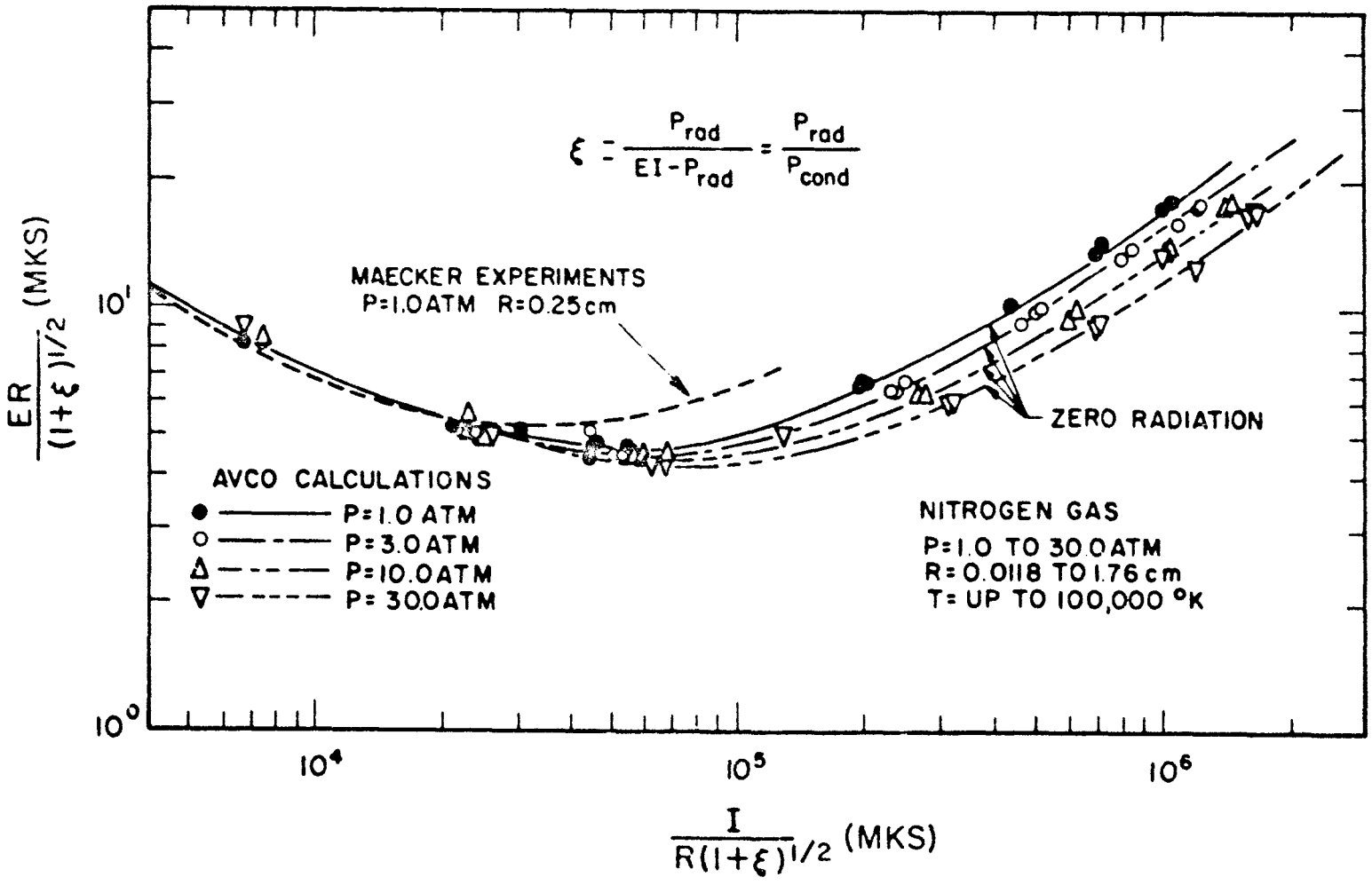

FIG. 17 CALCULATED NITROGEN CHARACTERISTICS PLOTTED WITH SIMILARITY VARIABLES INCLUDING RADIATION

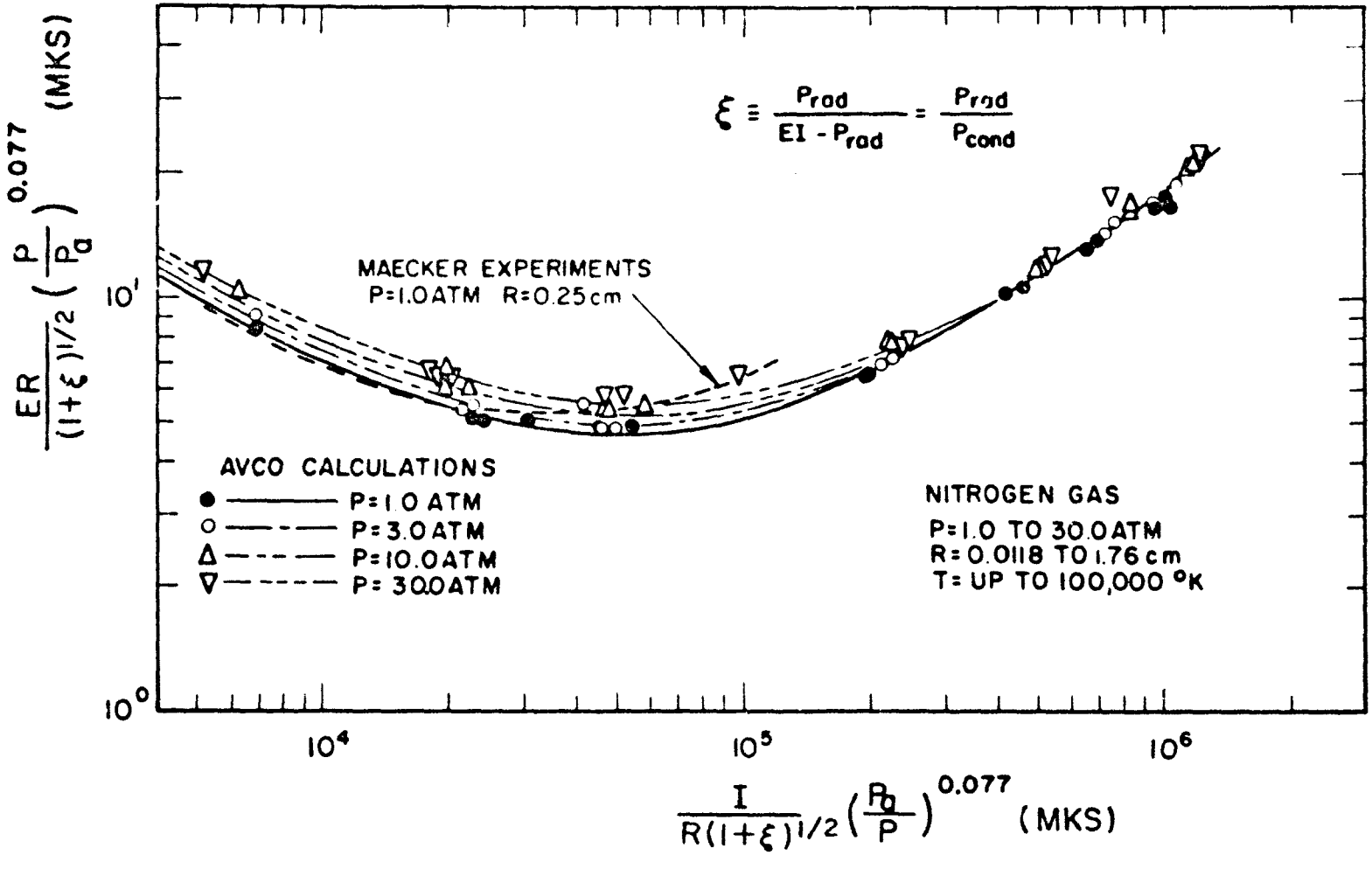

FIG. 18 CALCULATED NITROGEN CHARACTERISTICS PLOTTED WITH SIMILARITY VARIABLES INCLUDING RADIATION AND PRESSURE

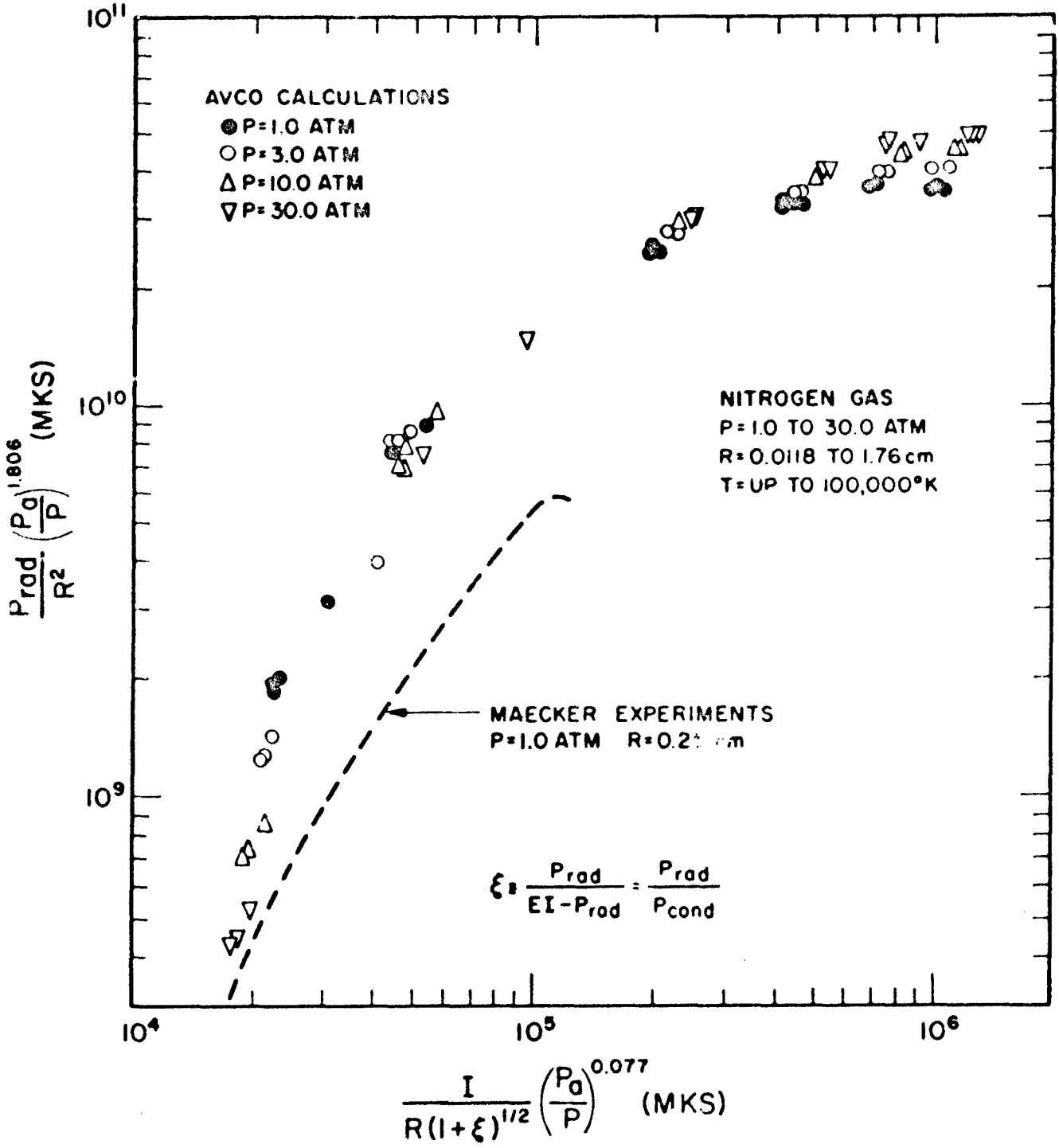

FIG. 19 CALCULATED NITROGEN RADIATION PLOTTED WITH SIMILARITY VARIABLES INCLUDING RADIATION AND PRESSURE

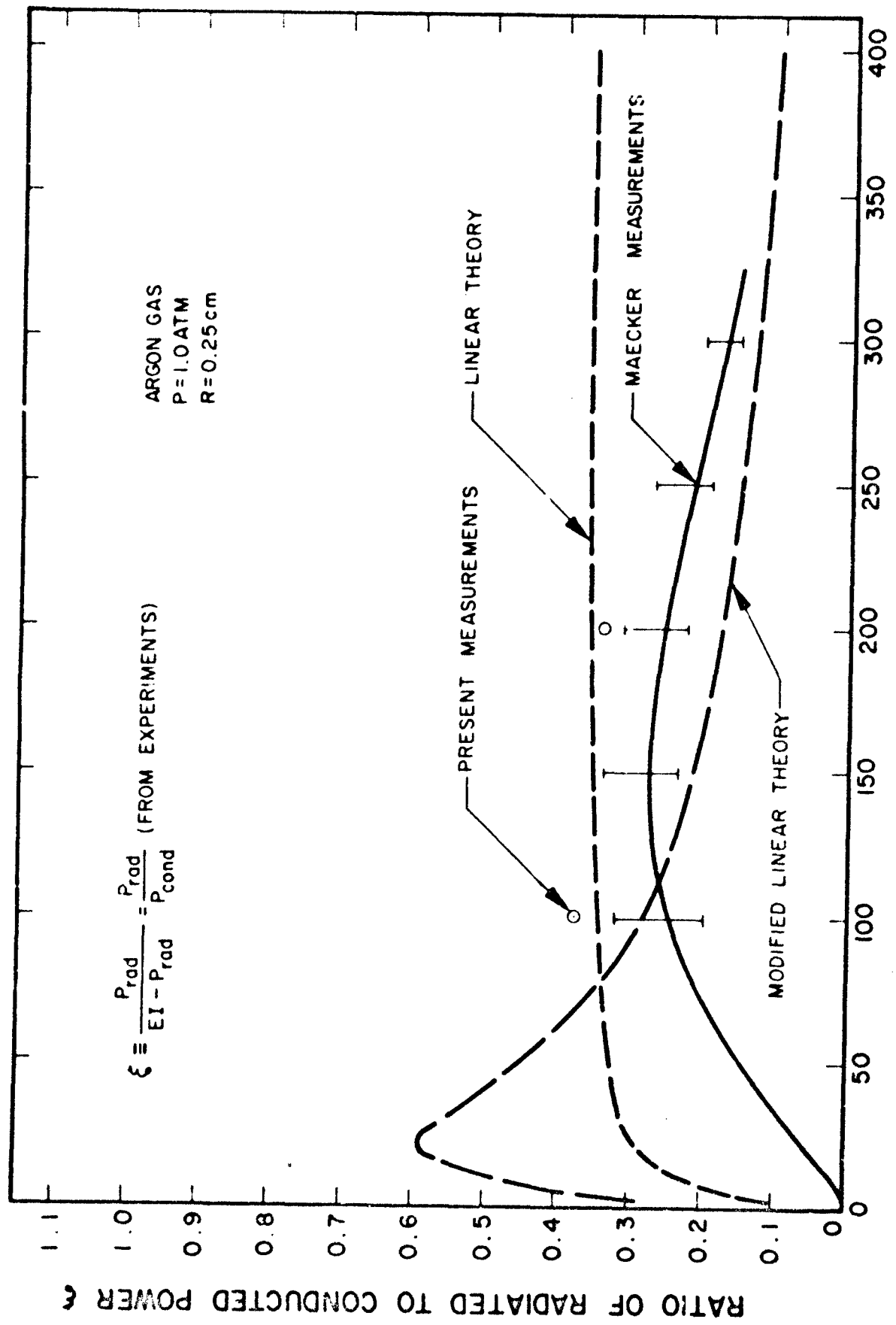

FIG. 20 RATIO OF RADIATED TO CONDUCTED POWER AS A FUNCTION OF CURRENT - ARGON GAS

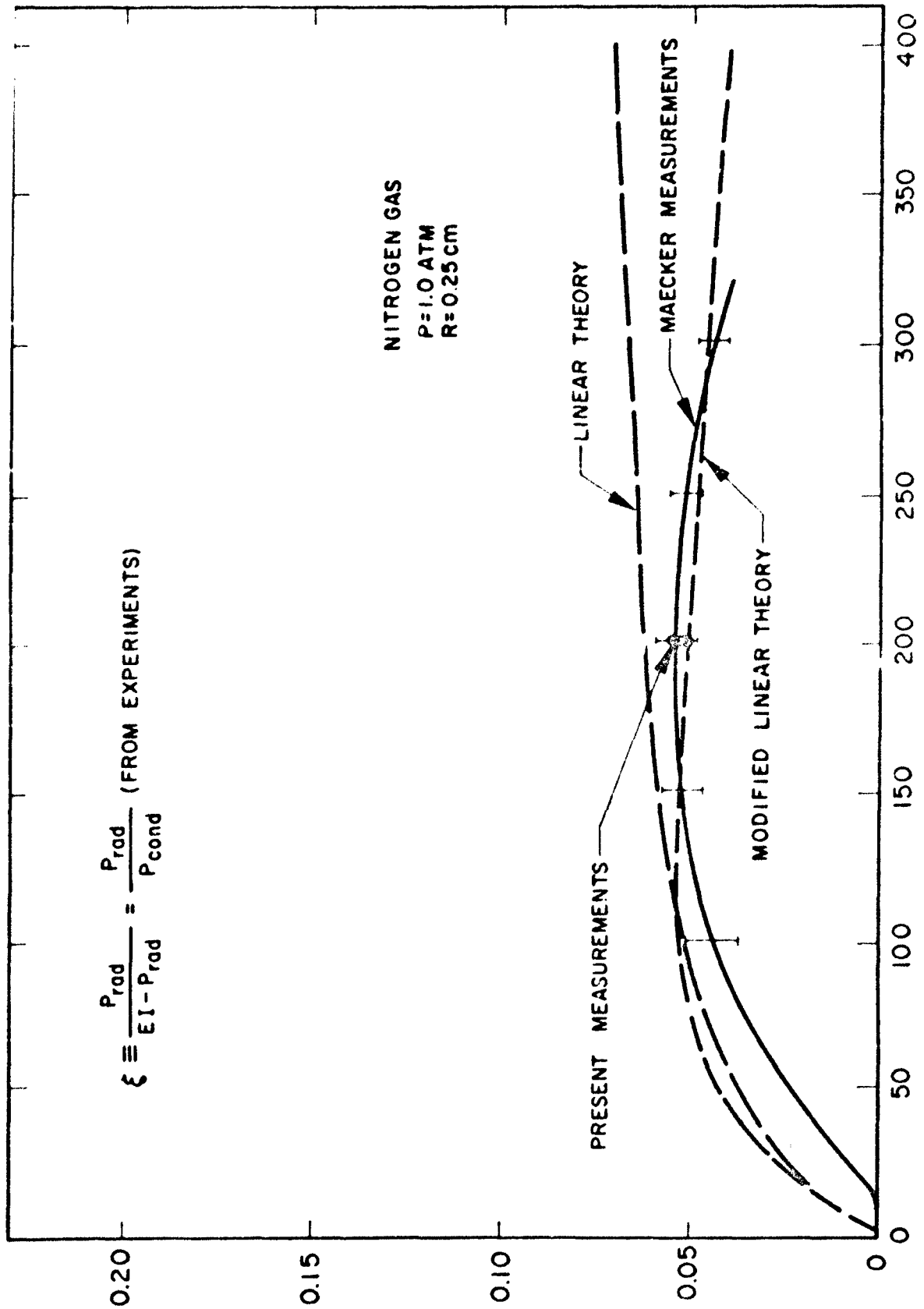

FIG. 21 RATIO OF RADIATED TO CONDUCTED POWER AS A FUNCTION OF CURRENT - NITROGEN GAS

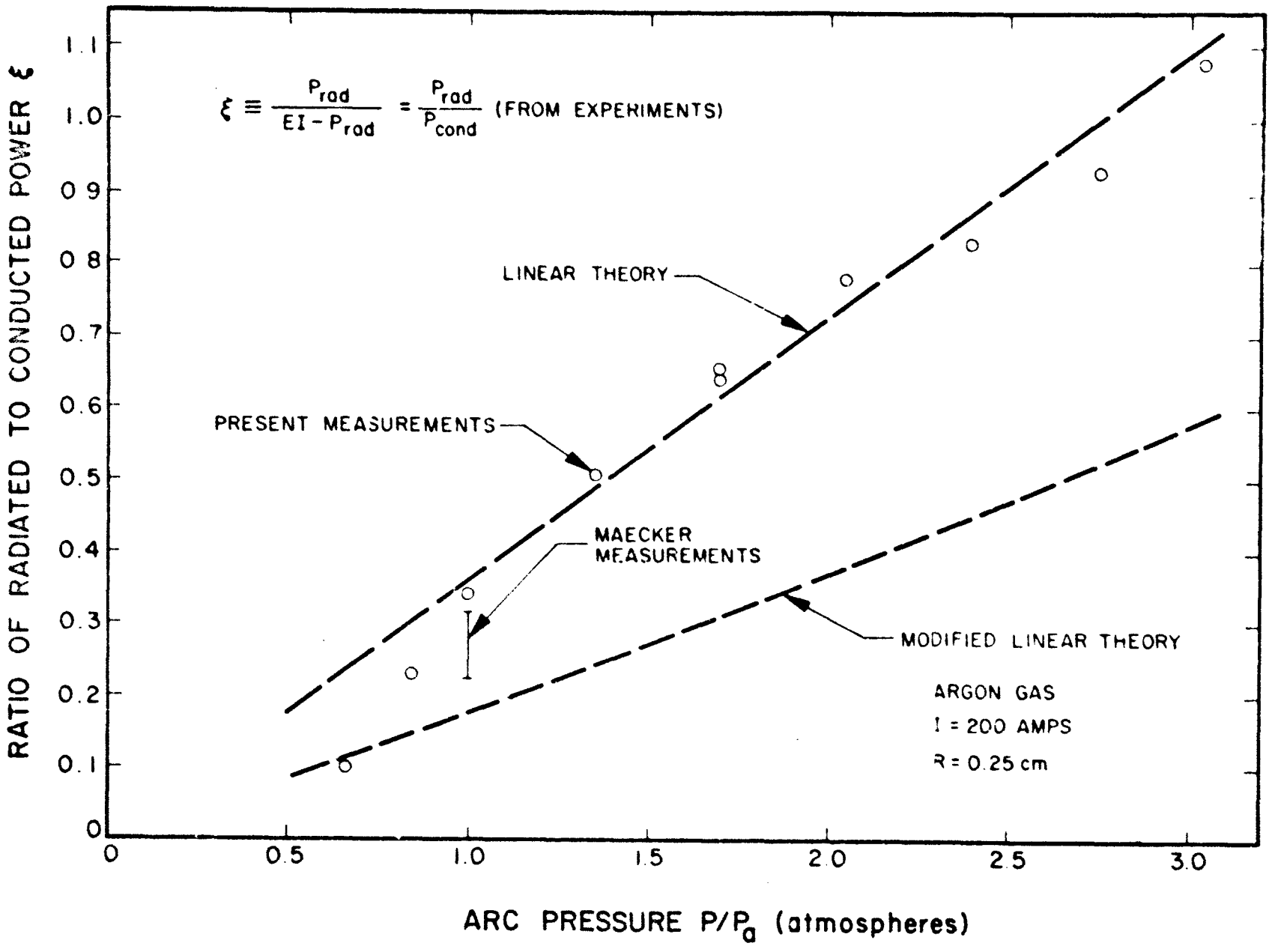

FIG. 22 RATIO OF RADIATED TO CONDUCTED POWER AS A FUNCTION OF PRESSURE - ARGON GAS

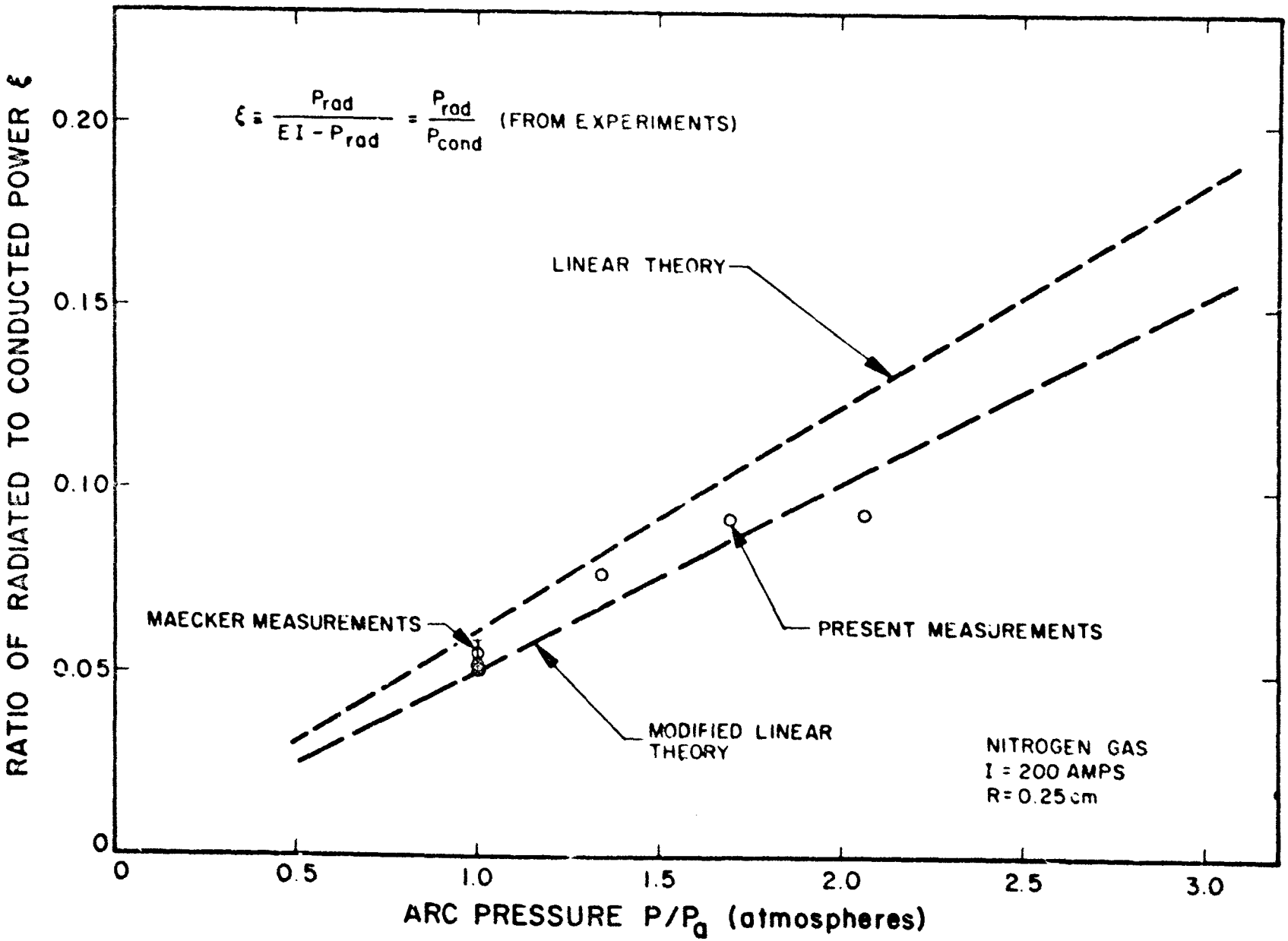

FIG. 23 RATIO OF RADIATED TO CONDUCTED POWER AS A FUNCTION OF PRESSURE - NITROGEN GAS